Journal of Neuroinflammation

RESEARCH

Open Access

PPARγ activation ameliorates cognitive impairment and chronic microglial activation in the aftermath of r-mTBI

Andrew Pearson[1,2*], Milica Koprivica[1], Max Eisenbaum[1,2], Camila Ortiz[1,2], Mackenzie Browning[1], Tessa Vincennie[1], Cooper Tinsley[1], Michael Mullan[1], Fiona Crawford[1,2,3] and Joseph Ojo[1,2,3]

Abstract

Chronic neuroinflammation and microglial activation are key mediators of the secondary injury cascades and cognitive impairment that follow exposure to repetitive mild traumatic brain injury (r-mTBI). Peroxisome proliferator-activated receptor-γ (PPARγ) is expressed on microglia and brain resident myeloid cell types and their signaling plays a major anti-inflammatory role in modulating microglial responses. At chronic timepoints following injury, constitutive PPARγ signaling is thought to be dysregulated, thus releasing the inhibitory brakes on chronically activated microglia. Increasing evidence suggests that thiazolidinediones (TZDs), a class of compounds approved from the treatment of diabetes mellitus, effectively reduce neuroinflammation and chronic microglial activation by activating the peroxisome proliferator-activated receptor-γ (PPARγ). The present study used a closed-head r-mTBI model to investigate the influence of the TZD Pioglitazone on cognitive function and neuroinflammation in the aftermath of r-mTBI exposure. We revealed that Pioglitazone treatment attenuated spatial learning and memory impairments at 6 months post-injury and reduced the expression of reactive microglia and astrocyte markers in the cortex, hippocampus, and corpus callosum. We then examined whether Pioglitazone treatment altered inflammatory signaling mechanisms in isolated microglia and confirmed downregulation of proinflammatory transcription factors and cytokine levels. To further investigate microglial-specific mechanisms underlying PPARγ-mediated neuroprotection, we generated a novel tamoxifen-inducible microglial-specific PPARγ overexpression mouse line and examined its influence on microglial phenotype following injury. Using RNA sequencing, we revealed that PPARγ overexpression ameliorates microglial activation, promotes the activation of pathways associated with wound healing and tissue repair (such as: IL10, IL4 and NGF pathways), and inhibits the adoption of a disease-associated microglia-like (DAM-like) phenotype. This study provides insight into the role of PPARγ as a critical regulator of the neuroinflammatory cascade that follows r-mTBI in mice and demonstrates that the use of PPARγ agonists such as Pioglitazone and newer generation TZDs hold strong therapeutic potential to prevent the chronic neurodegenerative sequelae of r-mTBI.

Introduction

Traumatic brain injury (TBI) is a leading cause of mortality, morbidity, and disability in both developed and developing nations [54, 143]. TBI affects approximately 2.8 million people in the USA every year [124]. Even in injuries diagnosed as mild TBI (mTBI), it is estimated that between 10 and 40% of mTBI patients live with cognitive and functional impairments that may persist

*Correspondence:
Andrew Pearson
apearson@roskampinstitute.org
[1] The Roskamp Institute, 2040 Whitfield Avenue, Sarasota, FL 34243, USA
[2] The Open University, Walton Hall, Kents Hill, Milton Keynes MK7 6AA, UK
[3] James A. Haley Veterans' Hospital, 13000 Bruce B Downs Blvd, Tampa, FL 33612, USA

for months to years after injury [21, 78, 105]. Exposure to repeated mTBIs (r-mTBIs) sustained within a short time window can exacerbate the pathological and functional consequences of injury [6, 19, 23, 38]. Exposure to r-mTBI, often observed amongst military populations and athletes participating in high-contact sports is strongly associated with the development of later-life neurodegenerative pathologies seen histologically by the presence of neurofibrillary tangles of hyperphosphorylated tau and amyloid beta (Aβ) plaques [8, 70, 71, 73, 103, 104]. Despite this, there are no therapeutics available to clinicians to reduce the chronic sequelae of TBI and current treatment strategies are limited to symptom alleviation and rehabilitative care [120].

TBI is a dynamic disease process that is broadly separated into two distinct phases referred to as primary and secondary injury [72]. Primary injury is a direct consequence of the biomechanical forces imparted on the head that cause direct physical damage to tissues [51, 103, 104]. The damage of tissues such as vessels and axon tracts induced by the primary injury initiate a cascade of secondary injurious effects [116]. Secondary injury is more prolonged and widespread, involving pathophysiological mechanisms such as neuroinflammation, metabolic dysfunction, oxidative stress, and changes in synaptic plasticity and integrity [103, 104, 110]. Chronic microglial activation, a key component of neuroinflammation is one of the cardinal features observed following exposure to repetitive head trauma [31, 32, 81, 83, 84, 86, 96, 97, 100]. The chronic nature of the secondary injury cascade make it an opportunistic target for the successful treatment of post-TBI symptoms. However, the progression of these secondary injurious processes over time are complex and incompletely understood. Moreover, it remains unknown whether these biochemical cascades of events are reversible.

Peroxisome proliferator-activated receptor-γ (PPARγ), an isoform of the PPAR family, is a ligand-activated transcription factor that once activated, forms a heterodimer with retinoid x (RXR) and subsequently binds to DNA to regulate the expression of genes which are essential for various metabolic processes and cell differentiation [35, 129]. PPARγ is well expressed by microglia and myeloid cells in the CNS and PPARγ activation by agonists have also been shown to exert anti-inflammatory and anti-oxidant properties after brain injury or in models of neurodegenerative disorders such as Alzheimer's and Parkinson's diseases [9, 91, 93, 102, 123]. Our previous analyses of the chronic pathobiology of r-mTBI have identified the chronic dysregulation of PPARγ signaling as a potential therapeutic target [95]. In this study, we examine the effects of a delayed Pioglitazone treatment on cognitive and pathological outcomes such as microglial activation at the chronic stages of r-mTBI pathophysiology. To further examine how PPARγ activation affects microglial activation at the chronic stages of injury, we developed a microglial-specific model of PPARγ overexpression and examined the effects on the microglial transcriptomic phenotype following exposure to our r-mTBI paradigm.

Methods and materials

Culture and in vitro treatment of IMG cells

Adult mouse-derived IMG microglial cells (EF4001; Kerafast, Boston, MA, USA) were maintained in DMEM/F12 (Sigma-Aldrich) culture medium supplemented with 10% heat-inactivated fetal bovine serum (FBS001-HI Neuromics), 2 mM L-glutamine and 1% anti-biotic & anti-mycotics. Cells were maintained at 37 °C and 5% CO_2 in a humidified culture incubator. The immortalized microglial (IMG) cell line was first characterized by McCarthy et al. [68]. These cells have been shown to more accurately recapitulate the in vivo microglial phenotype compared to other microglial cell lines such as BV2 cells [37, 58, 68, 69]. IMG cells were seeded into 24 well culture plates 24 h before exposure to Lipopolysaccharide (LPS) or Pioglitazone. Cells were incubated with control media, media containing only LPS (10 ng/ml), or media containing LPS (10 ng/ml) and Pioglitazone (10 μM) for 24 h.

Animals

Male C57BL6J mice at 12 weeks of age were obtained from Jackson laboratories (Bar Harbor, ME).

To generate the microglial-specific conditional overexpression of PPARγ mice, we crossed homozygous Flox-PPARγ-VP16$^{(+/+)}$ mice previously described by Kleinhenz and colleagues [59], with homozygous CX3CR1 CreERT2 EYFP reporter mice (Jackson Laboratories, #021160) to generate hemizygous CX3CR1$^{+/CreERT2}$- PPARγ-VP16$^{(+/fl)}$ (mcg-PPARγ^{OE}) mice. Hemizygous mcg-PPARγ^{OE} and homozygous CX3CR1$^{CreERt2+/+}$ (Cre genotype control) mice were used for experimental studies. Both male and female mice were used in each group in an approximate 50:50 ratio. The PPARγ-VP16 mice were a generous gift from Dr. Michael Hart.

Animals were housed in groups of three to four per cage under standard laboratory conditions (23 ∘C ± 1 °C, 50 ± 5% humidity, 14-hour light/10-h dark cycle) with ad libitum access to food and water throughout the study. All procedures involving mice were carried out under Institutional Animal Care and Use Committee approval and in accordance with the National Institutes of Health Guide for the Care and Use of Laboratory Animals.

Genotyping

Genotyping for Cre recombinase, CX3CR1, and PPARγ-VP16 was performed by Transnetyx, using tail snips as previously described by Jackson Labs [126].

Injury protocol

The r-mTBI paradigm was administered as previously described [100]. Briefly, all mice were anesthetized with 1.5 L/min of oxygen and 3% isoflurane prior to r-mTBI or sham injury. Once anesthetized, mice had their heads shaved, but no incisions were made. Mice were subsequently placed in a stereotaxic frame (Just for Mice™ Stereotaxic, Stoelting, Wood Dale, IL) mounted with an electromagnetic controlled impact device (Impact One™ Stereotaxic Impactor, Richmond, IL). The stereotaxic frame was fitted with a heating pad to maintain body temperature at 37 °C, and non-invasive rubber pads were fixed in place on either side of the head to prevent lateral movement during impact. A 5 mm blunt metal impactor tip was positioned above the sagittal suture before each impact. Injury was delivered to the closed skull with an impact velocity of 5 m/s, strike depth of 1.0 mm, and dwell time of 200 ms; the force applied to the mouse head at the time of impact is approximately 72 N under these conditions. All mice experienced short-term apnea (< 20 s) and showed no presence of skull fractures. All mice were then allowed to recover on a heating pad until the mouse became ambulatory and subsequently returned to their cages with access to soft food and water. Mice assigned to the r-mTBI cohort underwent this injury protocol daily with a 24-h inter-injury interval (5 hits/week, Monday to Friday) for a total of 20 injuries. To control for the effects of repeated anesthesia, mice assigned to the sham group underwent the same anesthesia protocol but did not receive an injury. Throughout the injury protocol and following injury, mice were monitored daily for any health concerns or behavioral abnormalities.

Pioglitazone treatment

Pioglitazone hydrochloride (#P1901) was purchased from TCI America and processed into standard soy protein free rodent chow (#TD190035) (Teklad, Envigo) at 12.5 ppm and 50 ppm. Pioglitazone doses were selected based on allometric scaling of commonly prescribed human doses [88]. Following treatment, all animals were euthanized 24 h after the final administration.

Tamoxifen treatment

Mcg-PPARγ^{OE} and CX3CR1$^{CreERt2+/+}$ mice were treated with 50 mg/kg (I.P) tamoxifen treatment for 5 consecutive days starting at 8 weeks of age. Following tamoxifen treatment, a four week "wash-out" phase was performed to allow for the turnover of peripheral monocytes before exposure to the r-mTBI paradigm.

Behavioral analysis

Barnes maze (BM) was performed to assess spatial learning and memory. Beginning 7 days before the start of the BM trials, mice were handled daily to reduce the potential effect of novel stressors on mouse behavior. BM was initiated 8 days before euthanasia and lasted for 7 consecutive days. During each day of Barnes maze testing all mice were carefully transferred from the vivarium to the behavioral analysis suite, at which point the cages were left undisturbed for 30 min to allow the animals time to recover from stress. The walls of the BM room were equipped with visual spatial cues which were kept constant for all 7 days, room lighting, and motivation to escape the maze was provided by high intensity LED floodlights and again were kept constant across all 7 days of testing. For the first 6 days (Acquisition phase), animals were trained to locate a target hole with a black escape box securely fixed underneath. The BM arena was a white polymer table 1.2 m in diameter with 18 equally spaced holes around its perimeter. Before beginning behavioral analysis, a still image of the BM table was taken and stored in the Noldus Ethovision XT visual tracking software. A mask was generated defining the target hole and all incorrect holes. This mask was overlayed onto a live camera image to enable the quantification of number of errors. Mice performed 4 trials per day during the acquisition phase, each lasting 90 s. The starting position of each trial was rotated, beginning at one of four cardinal positions (North, East, South, West) of the maze rotating clockwise. If an animal was unsuccessful in locating the target box or escaping the maze, animals were gently guided to the target hole by hand. Regardless of success, all mice spent 30 s in the escape box before returning to their cage. On day 7 (Probe phase), the escape box was removed, mice were placed in the middle of the maze and had 60 s to locate the correct hole.

Euthanasia

Mice were anesthetized with 1.5 L/min of oxygen and 3% isoflurane and were then perfused transcardially with phosphate-buffered saline (PBS), pH 7.4. Following perfusion, brains were either placed in a sterile petri dish for glial isolation, post-fixed in a solution of 4% paraformaldehyde (PFA) at 4 °C for 48 h and paraffin-embedded for immunohistochemistry, or flash frozen in liquid nitrogen and then stored at − 80 °C for subsequent biochemical analysis.

Tissue processing and immunohistochemistry

Brain samples fixed in PFA were paraffinized using the Tissue-Tek VIP (Sakura, USA). Sagittal sections were cut at 6 µm using a Leica RM2235 microtome and mounted on positively charged glass slides. Prior to staining, sections were deparaffinized in xylene and rehydrated in sequential ethanol solutions of decreasing concentration.

Immunohistochemical staining for Iba1, CD68, and GFAP

Reactive microglia and astrocytes were stained using anti-Iba1 (Wako) or anti-CD68 (Cell Signaling #97778s) and anti-GFAP (Dako) antibodies, respectively. Following tissue rehydration, slides were sub-merged in hydrogen peroxide for 15 min to remove endogenous peroxidases, followed by antigen retrieval in citric acid buffer (pH 6.0). Slides were then blocked with normal goat serum raised at room temperature for 1 h and subsequently incubated with primary antibody (Iba1-1:1000, GFAP-1:5000) at 4 ∘C overnight. The next day, slides were washed three times in PBS and incubated with their respective secondary antibody (VectaSTAIN ABC Kit) and developed using 3,3′-Diaminobenzidine (DAB).

Imaging

Imaging of Iba1, CD68, and GFAP was performed on an Olympus DP72 microscope at 20× magnification for the cortex and hippocampus, and 40× magnification for the corpus callosum. Three non-overlapping regions of interest (ROI) per section were selected for the hippocampus, the body of the corpus callosum, and the cortex (under the injury site). ROI were selected in identical brain regions regardless of the presence or absence of any pathological signs. Images were subsequently analyzed using the optical segmentation tool in ImageJ. Images were separated into individual color channels (hematoxylin counterstain and DAB chromogen) using a color deconvolution algorithm. Reactive coverage area was analyzed in mm^2 and were subsequently calculated as a percentage (%) of total area for each image. The mean values for each region and mouse were used for statistical analysis. Imaging and image analysis were performed by individuals who were blinded to the study groups.

Microglial isolation

Following transcardial perfusion of mice during euthanasia, mice were decapitated. The brain was removed, rinsed in PBS, and placed into a Petri dish on ice. Enzymatic tissue digestion was performed using the Adult Brain Dissociation Kit (130-107-677, Miltenyi Biotec) as previously described [29, 100]. Briefly, after removing the meninges, the brain was cut into small pieces using a sterile scalpel blade, and samples were transferred to a 15 mL tube where 1950 µL of enzyme mix 1 (enzyme P and buffer Z) and then 30 µL of enzyme mix 2 (enzyme A and buffer Y) were added, and brains were incubated in the enzyme mix for 30 min. Brains were then further digested using repeated trituration. Samples were briefly centrifuged and filtered through a 70 µm cell strainer to achieve a single-cell suspension. Single cells were resuspended in 900 µL of Debris removal solution and mixed with 3.1 mL of PBS containing 0.5% fetal bovine serum (FBS) (PB buffer), samples were then transferred to a fresh 15 mL falcon tube, and 4 mL of PB buffer was carefully overlayed. Samples were then centrifuged at 3000×*g* for 10 min. Cells were rinsed with PB buffer to remove any remaining debris removal solution and centrifuged for 10 min. The supernatant was aspirated, and cells were labeled with anti-CD11b magnetic particles for 10 min at 4 °C; the sample was then loaded onto a pre-conditioned LS separation column (130–042-401, Miltenyi Biotec) and rinsed three times to remove unlabeled cells. To elute $CD11b^{+ve}$ cells, the LS column was removed from the magnet, and PB buffer was used to elute the sample.

Nuclear protein isolation

Nuclear protein isolation was performed using the NE-PER nuclear and cytoplasmic extraction reagent kit (Thermo Scientific) according to manufacturer instructions. Isolated $CD11b^{+ve}$ cells were centrifuged for 5 min at 500×*g* to pellet cells. 100 µL of ice-cold cytoplasmic extraction reagent 1 (CER1) supplemented with protein-ase and phosphatase inhibitors (Thermo Scientific) was added to all samples. Samples were then mixed vigorously and incubated on ice for 10 min. 5.5 µL cytoplasmic extraction reagent 2 (CER2) was added to all samples, which were subsequently vortexed and centrifuged at 16,000×*g* for 5 min at 4 °C to separate nuclear and cytoplasmic proteins. The supernatant (cytoplasmic fraction) was transferred to a fresh tube and stored at − 80 °C. The pellet (nuclear fraction) was re-suspended in 50 µL of chilled nuclear extraction reagent (NER) and incubated on ice for 40 min with intermittent mixing (15 s every 10 min). The nuclear fraction was then centrifuged at 16,000×*g* for 10 min at 4 °C to remove insoluble material and the supernatant was transferred to a fresh tube and stored at − 80 °C.

Transcriptional activity assay

Analysis of PPARγ transcriptional activity was assessed using PPAR gamma Transcription Factor Assay Kit (ab133101, Abcam) and nuclear protein extracts from $CD11b^{+ve}$ cells. Assay was performed according to manufacturer instructions. 90 µL of complete transcription factor binding assay buffer (CTFB) and 10 µL of sample nuclear extracts was added to each well (90 µL of CTFB and 10 µL of manufacturer supplied positive control

sample was added to control wells). Samples were incubated overnight at 4 °C, the following morning wells were washed five times with 200 µL of 1X wash buffer and 100 µL of PPARγ primary antibody was added to appropriate wells. Samples were incubated with primary antibody for one hour at room temperature without agitation, then washed five times with 200 µL of 1X wash buffer. 100 µL of secondary was then added to appropriate wells, followed by a one-hour incubation at room temperature. Samples were again washed five times with 200 µL of 1X wash buffer and 100 µL of developing solution was added to all wells. Samples were incubated in the dark for 45 min at room temperature and 100 µL of stop solution was added to all wells and were immediately read at 450 nm using a Cytation 3 (Biotek, Winooski, VT) plate reader. Following quantification, all data were normalized to protein content of sample lysates, determined by Bicinchoninic acid (BCA) protein assay (ThermoFisher, Waltham, MA).

Cytokine quantification

Cytokine levels from isolated CD11b^{+ve} cells (n = 4/group) were analyzed using the V-PLEX proinflammatory Panel 1 mouse cytokine kit (MSD, Rockville, MD) according to the manufacturer's instructions. Briefly, samples were diluted 1:2 in Diluent 41 and incubated at room temperature for 2 h. Wells were washed to remove unbound analyte; secondary antibody was added, and the samples were left to incubate at room temperature for 1 h and quantified using the MESO QuickPlex SQ120 plate reader. Following quantification, all data were normalized to the protein content of sample lysates, determined by Bicinchoninic acid protein assay (ThermoFisher, Waltham, MA).

Immunoblotting

For immunoblotting analysis, isolated CD11b^{+ve} cells were homogenized in MPER supplemented with protease and phosphatase inhibitors (ThermoFisher) using a probe sonicator. Homogenized samples were centrifuged at 21,000 × *g* for 20 min at 4 °C, and the supernatant was transferred to a fresh Eppendorf tube. Supernatant fractions were denatured by boiling at 95 °C for 10 min in Laemmli buffer (Bio-Rad) containing β-mercaptoethanol. Samples were then resolved on a 4–15% gradient polyacrylamide criterion gel (Bio-Rad). Proteins were then transferred to a Polyvinylidene Fluoride (PVDF) membrane (BioRad) overnight at 90 mAh. Transferred membranes were blocked in a 5% non-fat milk buffer in Tris-buffered saline (TBS) containing 0.05% sodium azide (NaN3) for 1 h at room temperature and then incubated with different target-specific primary antibodies overnight. The following primary antibodies were used: anti-NLRP3 (1:1000, Adipogen, #AG-20B-0014-C100), anti-Phospho STAT3(Tyr705) (1:1000, Cell signaling, #9145), anti-STAT3 (1:1000, Cell signaling, #4904), anti-Phospho NFκB(Ser536) (1:1000, Cell signaling, #3033 s), anti- NFκB (1:1000, Cell signaling, #8242 s), anti-PPARγ (1:500, ThermoFisher, #PA3-821A), anti-PGC1α (1:1000, Novus Bio, NBP1-0676SS), anti-Tubulin (1:1000, Cell signaling, #2144), anti-β actin (1:1000, Cell signaling, #4967).

RNA isolation

RNA isolation from isolated cells was performed as previously described [29]. Briefly, 500µL of TRIzol (Fisher Scientific, Waltham, MA) was added under RNase free conditions to isolated CD11b + ve cells (N = 4–5/group), and cells were lyzed through trituration. Following homogenization, samples were incubated at room temperature for 5 min to allow for dissociation of nucleoprotein complexes and 100 µL of 1-bromo-3-chloropropane reagent (Sigma, St. Louis, MO) was added to each sample. Samples were briefly vortexed and centrifuged at 12,000×*g* for 15 min. The aqueous phase was carefully removed, and the organic phase was transferred to a fresh eppendorf tube and stored at − 80 °C for subsequent protein precipitation. 20 ng of ultrapure glycogen (Fisher Scientific, Waltham, MA # AM9510) was added, samples were again briefly mixed, and RNA was subsequently precipitated using 500 µL of ice-cold 100% Isopropanol. The RNA pellet was washed twice with 75% ethanol in Diethyl pyrocarbonate (DEPC) treated water (Fisher Scientific, Waltham, MA, R0601). Pellets were briefly air-dried and then resuspended in DEPC water, RNA concentrations (ng/µL) and RNA purity (260:280) were calculated using a Cytation 3 (Biotek, Winooski, VT). At least 500 ng/sample of RNA were sent to Azenta LLC (South Plainfield, NJ, USA) for subsequent RNA library preparation and total RNA sequencing (20–30 million reads). RNA samples received by Azenta LLC were quantified using Qubit 2.0 Fluorometer (LifeTechnologies, Carlsbad, CA, USA) and RNA integrity was checked using Agilent TapeStation 4200 (Agilent Technologies, Palo Alto, CA, USA).

RNA sequencing

Full details of RNA library preparation can be obtained from Azenta LLC (South Plainfield, NJ, USA). Briefly, RNA sequencing libraries were prepared using the NEBNext Ultra RNA Library Prep Kit for Illumina using manufacturer's instructions (NEB, Ipswich, MA, USA). Briefly, mRNAs were initially enriched with Oligo(dT) beads. Enriched mRNAs were fragmented for 15 min at 94 °C. First and second strand cDNA were subsequently synthesized. cDNA fragments were end repaired

and adenylated at 3'ends, and universal adapters were ligated to cDNA fragments, followed by index addition and library enrichment by PCR with limited cycles. The sequencing library was validated on the Agilent TapeStation (Agilent Technologies, Palo Alto, CA, USA), and quantified by using Qubit 2.0 Fluorometer (Invitrogen, Carlsbad, CA) as well as by quantitative PCR (KAPA Biosystems, Wilmington, MA, USA). The sequencing libraries were clustered on a single lane of a flow cell. After clustering, the flowcell was loaded on the Illumina HiSeq 4000 according to manufacturer's instructions. The samples were sequenced using a 2×150 bp Paired End (PE) configuration. Image analysis and base calling were conducted by the HiSeq Control Software (HCS). Raw sequence data (.bcl files) generated from Illumina HiSeq were converted into fastq files and de-multiplexed using Illumina's bcl2fastq 2.17 software. One mismatch was allowed for index sequence identification.

Bioinformatics

Bioinformatic processing was performed as previously described [29]. Breifly, sequencing data were uploaded to the galaxy web platform, and the public server usegalaxy.org was used to analyze the data [1]. Raw data in the fastq format were first pre-processed using the sample quality control (QC) program FastQC [3], QC data were then aggregated using MultiQC [30]. All data were then processed through Trimmomatic [11], to remove adapter sequences, poly-N-containing reads, and low-quality reads (Phred score < 25). Paired end reads were then aligned to the mouse genome using HiSAT2 and the GRCm38 (mm10) mouse reference genome [57]. Duplicate reads were removed, and gene expression in FPKM (Fragments Per Kilobase Million) was measured using FeatureCounts [63]. Sample data were aggregated into a single data frame using column join, and gene IDs were annotated using the AnnotateMyIDs program [27]. Batch correction was performed using RUVSeq [107], and differential expression analysis was performed using the DESeq2 program [65]. Resulting p values were adjusted using the Benjamini and Hochberg approach to control for false discovery rate. Genes identified using DESeq2 that reported a false discovery rate corrected p value of < 0.05 were regarded as differentially expressed genes (DEGs).

Gene enrichment analysis

Data from all experiments were subsequently uploaded to Ingenuity pathway analysis (IPA, QIAGEN). Datasets were filtered for differentially expressed genes (FDR < 0.05), and both significantly up and downregulated genes were analysed together to identify enriched canonical pathways. The ingenuity knowledge base was used as a reference set to identify significantly enriched pathways following analysis by Fisher's exact test and the activation or inhibition of enriched pathways was determined with the use of a Z-score.

Statistical analysis

GraphPad PRISM software (GraphPad Software Inc.) was used to generate the graphs and perform statistical analysis. The results are expressed as mean ± SEM. Statistical tests performed are stated in the corresponding figure legend.

Results

Pioglitazone treatment inhibits LPS-induced microglial NF-κB activation in vitro

PPARγ activation has been suggested to exert anti-inflammatory effects on microglia and macrophages. As such, we hypothesized that prolonged PPARγ activation would ameliorate microglial activation and inflammatory signaling following r-mTBI. But first, we assessed the anti-inflammatory potential of PPARγ agonism in microglia, by exploring the effects of the well-known PPARγ agonist Pioglitazone on LPS-exposed immortalised microglia (IMG) in vitro. Following LPS exposure for 24 h, PPARγ transcriptional activity was significantly reduced compared to controls. However, co-administration of LPS and Pioglitazone to IMG cells prevented the LPS-induced decrease in PPARγ transcriptional activity (Fig. 1A). One such mechanism through which PPARγ is thought to reduce inflammation is via the inhibition of NFκB signaling [17, 24]. As such we examined the lysates of IMG cells exposed to either LPS (10 ng/mL), Pioglitazone (10 μM), or both for 24 h and assessed the effects on NFkB activation. As expected, LPS exposure alone significantly increased NFkB phosphorylation compared to control samples. In line with the Pioglitazone-induced increase in PPARγ transcriptional activity we observed that Pioglitazone treatment was able to significantly reduce the NFkB phosphorylation relative to cells treated with LPS alone (Fig. 1B).

Pioglitazone treatment ameliorates chronic deficits in spatial learning and memory

After observing prominent anti-inflammatory effects of Pioglitazone treatment in vitro, we next sought to assess how PPARγ agonism may influence the chronic outcomes of r-mTBI. To this end, mice were exposed to our 20-hit r-mTBI paradigm and were treated with either low (12.5 ppm) or high (50 ppm) Pioglitazone for 3 months starting at 3 months post injury. Seven days before the end of treatment mice underwent Barnes maze testing to assess spatial and learning memory (Fig. 2).

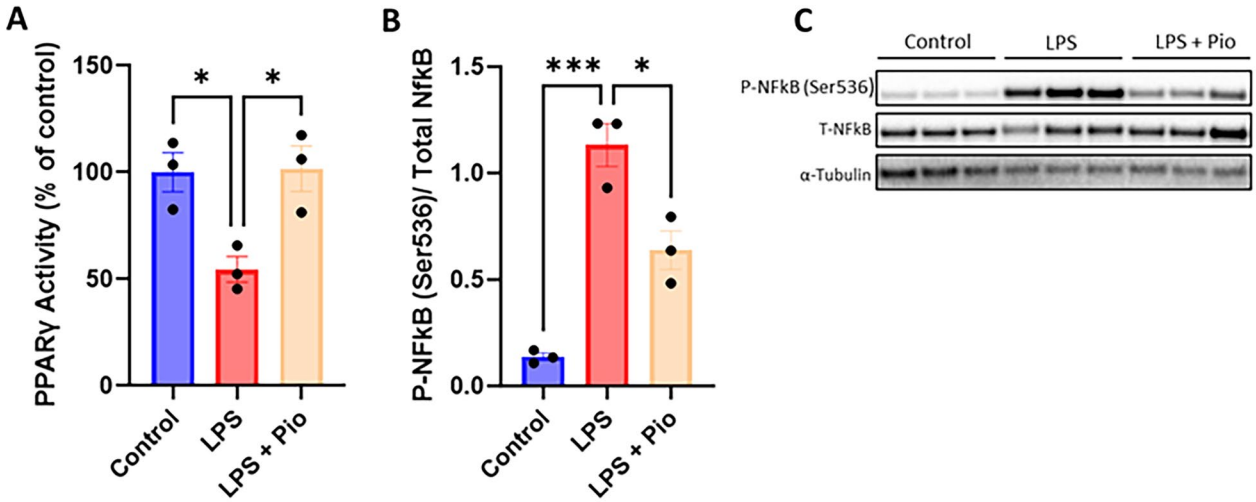

Fig. 1 PPARγ activation reduces the LPS-induced inflammatory response in microglia. Immortalised microglia (IMG) were exposed to LPS (10 ng/ml) or LPS (10 ng/ml) and Pioglitazone (10 μM) for 24 h before harvesting. **A** Assessment of PPARγ transcriptional activity in IMG cells following control, LPS, or LPS + Pioglitazone treatment. **B** Quantification of the Phosphorylated NFκB (Ser536) to total NFκB ratio in microglial cell lysates following exposure to control, LPS, or LPS + Pioglitazone treatment for 24 h. **C** Representative immunoblot image showing the protein expression of Phospho and total NFκB in microglia. α-Tubulin served as a loading control. Data were analyzed by a one-way ANOVA followed by Tukey's correction for multiple comparisons (n = 3/group). Asterisks denote statistical significance as follows: *p < 0.05, ***p < 0.001

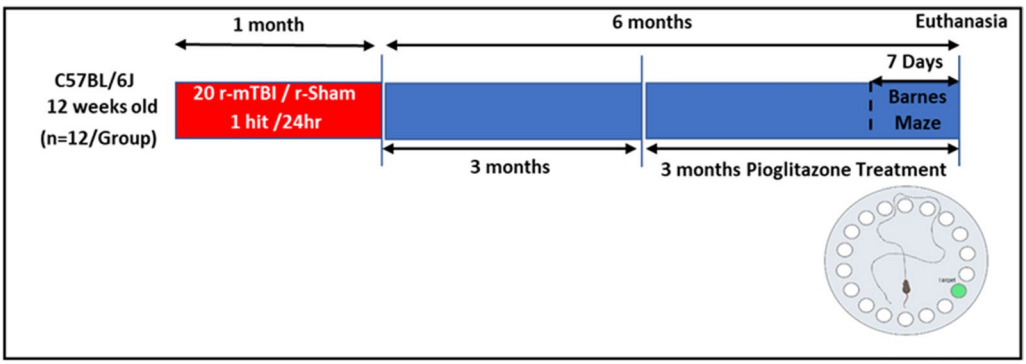

Fig. 2 Schematic representation of the experimental timeline. At 12 weeks of age, male C57BL6/J mice were exposed to our 20-hit r-mTBI paradigm consisting of five injuries per week for four weeks. Injuries were separated by 24 h. At three months post-last injury, sham and injured mice were randomly selected for low or high dose Pioglitazone treatment for three months. At one week prior to the end of treatment, spatial memory and learning function was assessed using the Barnes maze

Spatial learning was tested by assessing cumulative distance to the target hole (CD) over the 6-day acquisition phase (Fig. 3A). A three-way mixed ANOVA was run to investigate the effects of injury, treatment, and time on cumulative distance. At six months post-injury there was a statistically significant three-way interaction between treatment, r-mTBI, and time ($F(7.694, 42) = 3.285$, $p = 0.002$). Further analysis using a two-way ANOVA found a significant interaction of injury and treatment on spatial learning on days 3 ($F(2,62) = 4.099$, $P = 0.021$), 5($F(2,62) = 4.229$, $P = 0.019$), and 6 ($F(2,62) = 10.399$, $P \leq 0.001$) of the acquisition phase. Post-hoc analysis revealed a significant main effect of injury on day 3, and significant effects of injury and treatment days 5 and 6. We observed a greater recorded CD in r-mTBI animals who received either vehicle ($p = 0.011$) or low dose Pioglitazone ($p = 0.013$) treatment relative to their sham counterparts respectively. Pairwise comparison analysis revealed that injured animals treated with high dose Pioglitazone demonstrated a significantly reduced CD relative to injured animals who received vehicle treatment on both days 5 and 6. Interestingly, while Pioglitazone treatment had no significant effect on sham animals regardless of dose, we observed an indication of a dose–effect in r-mTBI animals, with those treated with high dose Pioglitazone

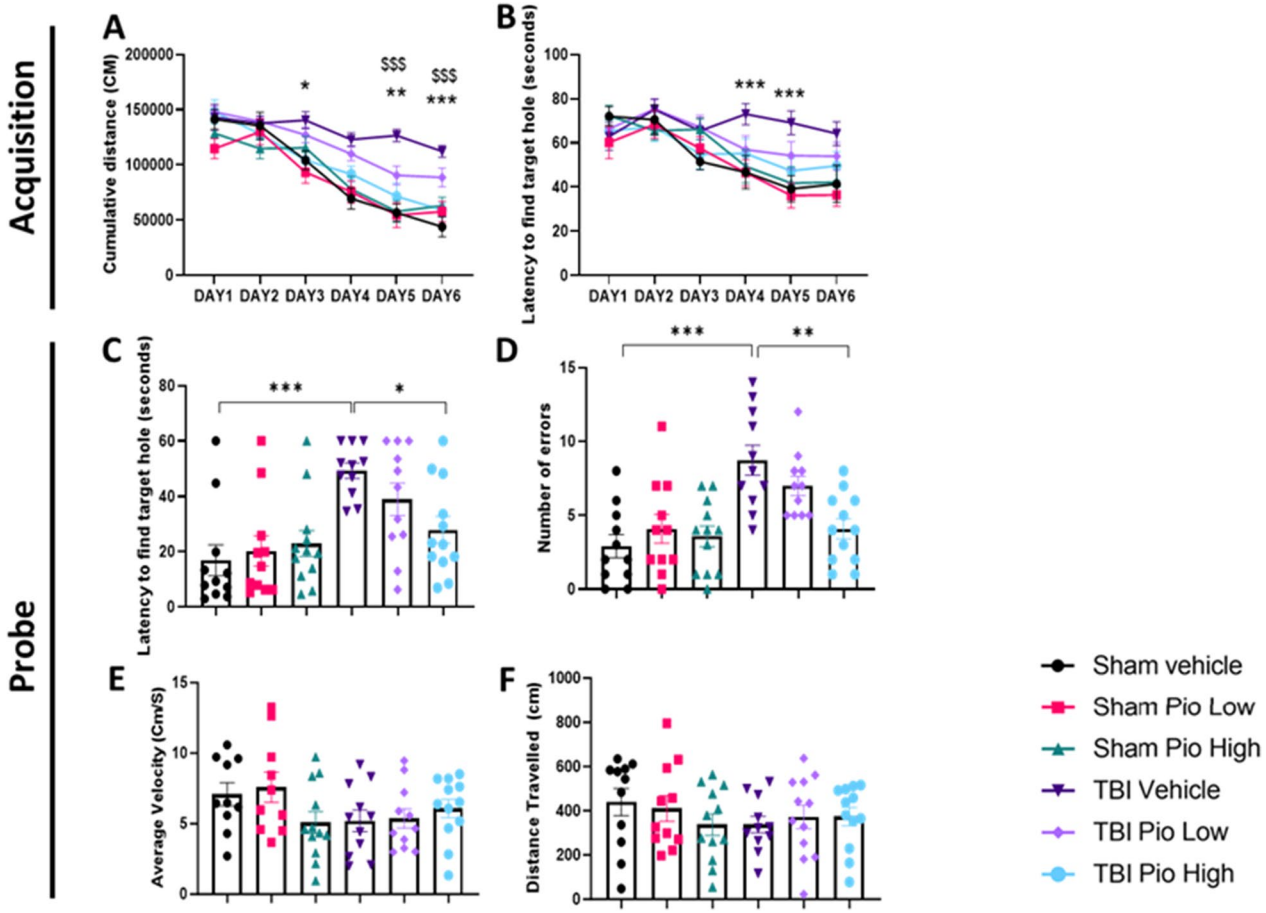

Fig. 3 PPARγ activation ameliorates r-mTBI associated memory and learning deficits. Acquisition data shows learning across the six acquistion phase by the mean cumulative distance to the target hole in cm (**A**), and the mean latency to find the target hole (**B**). Probe data shows the mean latency to find the target hole (**C**), number of errors (**D**), average velocity (**E**), and total distance traveled (**F**). Acquisition trials (**A**, **B**) were analyzed using a repeated measures three-way ANOVA followed by Tukey's correction for multiple comparisons (n = 10–12/group). Probe data (**C-F**) were analyzed using a two-way ANOVA followed by by Tukey's correction for multiple comparisons. Asterisks denote statistical significance between TBI vehicle and sham vehicle treated mice as follows: *$p < 0.05$, **$p < 0.01$, ***$p < 0.001$. $ denote statistical significance between TBI High dose and TBI vehicle treated mice as follows: $^{\$}p < 0.05$, $^{\$\$}p < 0.01$, $^{\$\$\$}p < 0.001$. Values are expressed as mean ± SEM

performing significantly better than low dose treated r-mTBI animals ($p = 0.025$).

Spatial learning and cognitive function were further assessed by recording the latency to first acquire the target hole (Fig. 3B). Mice exposed to our r-mTBI paradigm took significantly longer to locate the target hole compared to sham animals, but no significant effect of treatment was observed over the 6 day.

After 6 days of training, the hidden target box was removed, and spatial memory was assessed by their ability to locate the target hole using the visual clues in their environment. Consistent with our data from the acquisition phase, injured mice took significantly longer to find the target hole than their sham counterparts (Fig. 3C). Two-way ANOVA analysis found no significant main effect of treatment. However, a significant interaction between r-mTBI and treatment was recorded. Post-hoc analysis revealed that injured mice who received vehicle treatment took significantly longer to find the target hole than vehicle-treated sham animals ($p \leq 0.001$). While our data indicate that low dose Pioglitazone had no effect on latency to find the target hole, injured mice treated with high-dose Pioglitazone demonstrated a substantial reduction in target hole latency compared to vehicle-treated r-mTBI mice ($P = 0.039$). No significant difference was noted between injured mice treated with high-dose Pioglitazone and sham animals who received high-dose Pioglitazone ($P = 0.977$) or vehicle treatment ($P = 0.619$).

Notably, while some mice would acquire the target hole as expected, analysis of the footage indicated some mice would circle the maze moving from hole to hole in an attempt to locate the target box. Therefore, in addition to latency, we also analyzed number of entry errors (Fig. 3D). We observed that vehicle-treated injured mice

made significantly more errors during the probe trial than their vehicle-treated sham counterparts ($p \leq 0.001$). However, injured mice who received high dose Pioglitazone demonstrated a significant decrease in the number of errors relative to vehicle-treated r-mTBI mice ($p = 0.002$), indicating improved retention of spatial memory.

Throughout behavioral analysis, we recorded the average velocity and distance travelled to assess motor function (Fig. 3E, F). Statistical analysis found no significant effects of injury or treatment on average velocity or distance travelled suggesting exposure to r-mTBI does not induce motor deficits.

Pioglitazone treatment rescues chronic reactive gliosis

We have previously demonstrated that while exposure to our 20-hit r-mTBI paradigm does not induce gross neuronal loss, it does result in chronic reactive gliosis up to 3 months post-injury [100]. As inflammation is linked to behavioural impairments [7, 46], we examined the effect of Pioglitazone treatment on chronic microglia and astrocyte reactivity following r-mTBI. As behavioural testing found a limited effect of low dose Pioglitazone treatment, our subsequent analyses focused on the assessment of high dose Pioglitazone.

Brain tissue was collected at 6 months post-last injury, tissue sections were subsequently labeled with anti-Iba1, anti-CD68, and anti-GFAP and immunoreactive populations of microglia and astrocytes were quantified in the cortex (underneath the impact site), the hippocampus, and the corpus callosum. Building upon our prior work, we observed that exposure to r-mTBI induced a significant increase in Iba1 immunoreactivity in all three regions assessed (Fig. 4A–O). Treatment with Pioglitazone in injured mice resulted in a significant reduction in Iba1 in the hippocampus but showed no effect in the Cortex or Corpus Callosum. We next assessed the expression of the marker CD68, a lysosome-associated membrane protein which has been implicated in the regulation of phagocytic activity [34, 47]. We observed a significant injury-dependent increase in CD68 immunoreactivity in the Cortex, and Corpus Callosum which was significantly ameliorated following Pioglitazone treatment (Fig. 5A–O).

Our findings also demonstrate an impact of Pioglitazone treatment on reactive astrocyte populations in these brain regions. Specifically, we observed that exposure to r-mTBI induced a significant increase in GFAP immunoreactivity in Cortex, Hippocampus, and Corpus Callosum (Fig. 6A–O). However, r-mTBI mice treated with Pioglitazone demonstrated a significant decrease in GFAP immunoreactivity in all regions assessed suggesting that PPARγ agonism may be an effective target to reduce chronic reactive glial changes following r-mTBI.

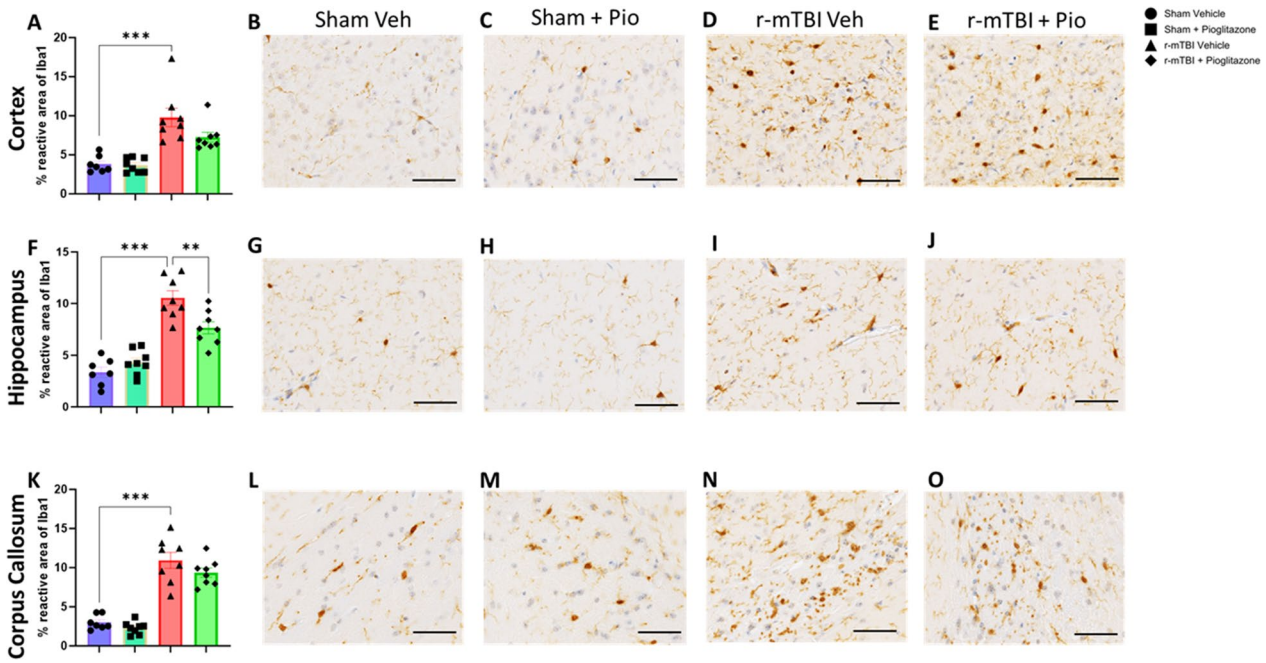

Fig. 4 Effect of PPARγ activation by Pioglitazone on microglial activation (Ionized calcium binding adaptor molecule 1 [Iba1]) at 6 months post r-mTBI. Quantitation and representative microscope images of $Iba1^{+ve}$ immunoreactive area in the cortex (**A**–**E**), hippocampus (**F**–**J**), and Corpus Callosum (**K**–**O**) (n = 7/8 per group). Data were analyzed using a two-way ANOVA followed by Tukey's correction for multiple comparisons. All data are expressed as mean ± SEM percentage reactive area

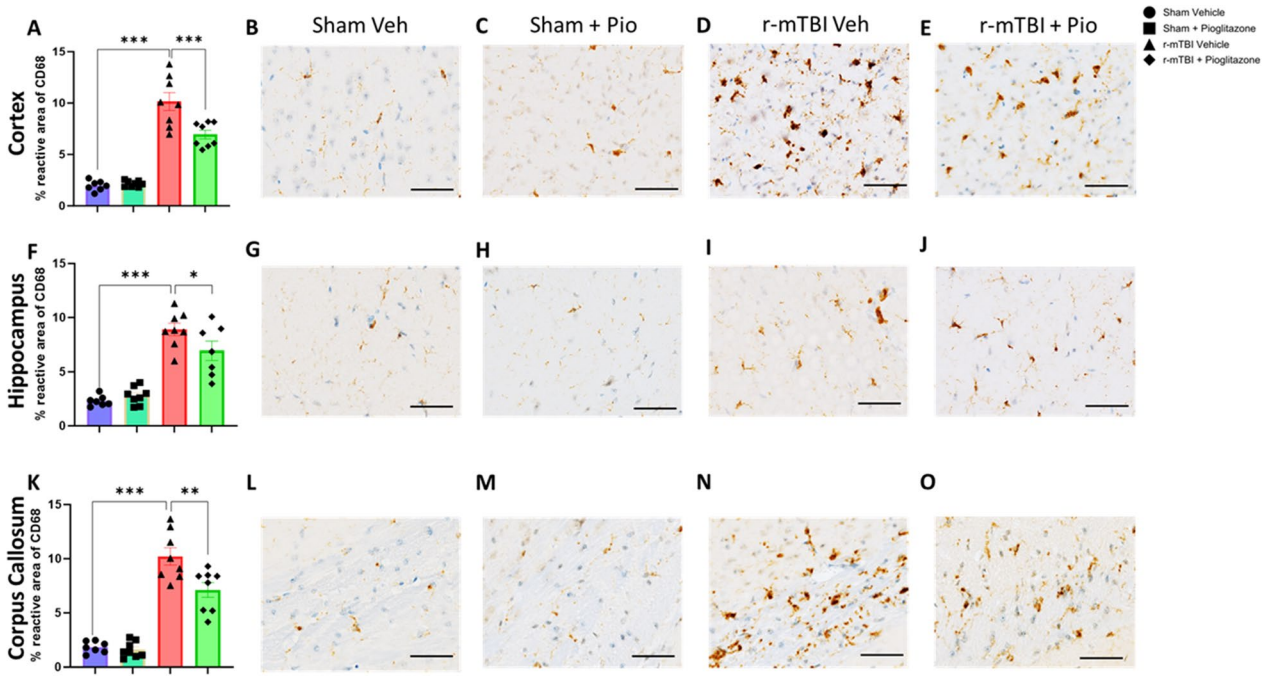

Fig. 5 Effect of PPARγ activation by Pioglitazone on microglial activation (Cluster of differentiation 68 [CD68]) at six months post r-mTBI. Quantitation and representative microscope images of $CD68^{+ve}$ immunoreactive area in the cortex (**A**–**E**), hippocampus (**F**–**J**), and Corpus Callosum (**K–O**) (n = 7/8 per group). Data were analyzed using a two-way ANOVA followed by Tukey's correction for multiple comparisons. All data are expressed as mean ± SEM percentage reactive area

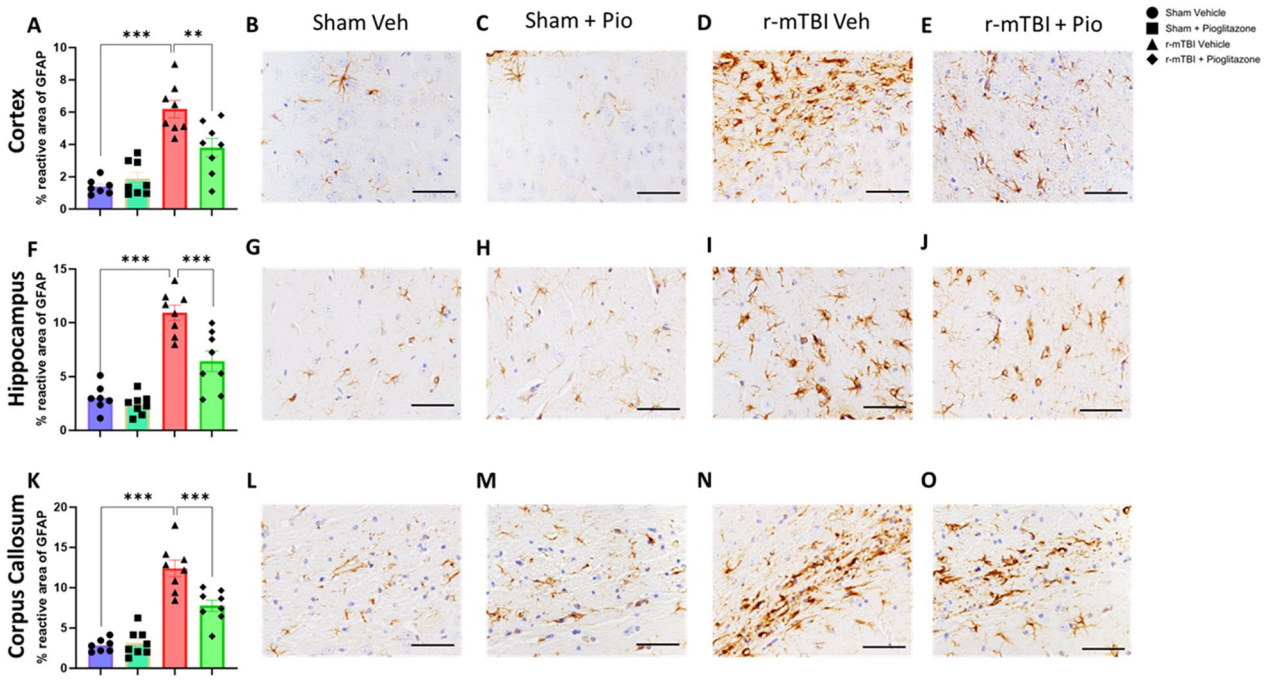

Fig. 6 Effect of PPARγ activation by Pioglitazone on astrocyte activation (Glial fibrillary acid protein [GFAP]) at six months post r-mTBI. Quantitation and representative microscope images of $GFAP^{+ve}$ immunoreactive area in the cortex (**A**–**E**), hippocampus (**F**–**J**), and Corpus Callosum (**K–O**) (n = 7/8 per group). Data were analyzed using a two-way ANOVA followed by Tukey's correction for multiple comparisons. All data are expressed as mean ± SEM percentage reactive area

Pioglitazone treatment rescues microglial PPARγ signaling

With promising evidence of beneficial effects observed during behavioral and neuropathological analyses, we next sought to better understand the microglial specific neuroinflammatory mechanism that drives r-mTBI pathophysiology and how PPARγ agonism via Pioglitazone treatment may beneficially influence these pathogenic cascades. Herein, we isolated $CD11b^{+ve}$ microglial cells from the brains of vehicle or Pioglitazone treated sham and injured mice at six months post-injury and assessed the activation of PPARγ signaling and inflammatory signaling pathways.

To assess how exposure to r-mTBI may affect microglial PPARγ signaling we assessed the DNA binding activity of PPARγ via transcriptional activity assay and quantified the expression of PPARγ and its co-factor PGC1α by immunoblotting. In line with our in vitro findings, PPARγ transcriptional activity was inhibited in microglia isolated from vehicle-treated r-mTBI mice relative to sham animals. However, we observed no effect of Pioglitazone treatment on brain myeloid cell specific PPARγ transcriptional activity in either sham or injured animals relative to their respective vehicle-treated controls (Fig. 7A).

We next asked if the changes in transcriptional activity also reflected changes in PPARγ protein expression. Immunoblotting revealed that PPARγ expression was reduced in microglia isolated from vehicle-treated r-mTBI mice relative to their sham vehicle-treated counterparts. Post-hoc analysis revealed that Pioglitazone treatment had no significant effect on PPARγ expression in sham animals relative to sham vehicle-treated controls. However, in injured animals, we observed that pioglitazone treatment markedly increased PPARγ expression relative to vehicle treated animals (Fig. 7B).

To further develop these findings, we assessed if the beneficial effects of Pioglitazone treatment observed may be mediated through changes in the protein expression of PGC1α (Fig. 7C). PGC1α is a transcriptional coactivator of PPARγ and has been implicated in the regulation of several genes associated with microglial polarization, neuroinflammation, and mitochondrial biogenesis. In accordance with our findings on PPARγ expression, we observed that microglial PGC1α expression was chronically reduced in mice exposed to r-mTBI but was rescued following Pioglitazone treatment.

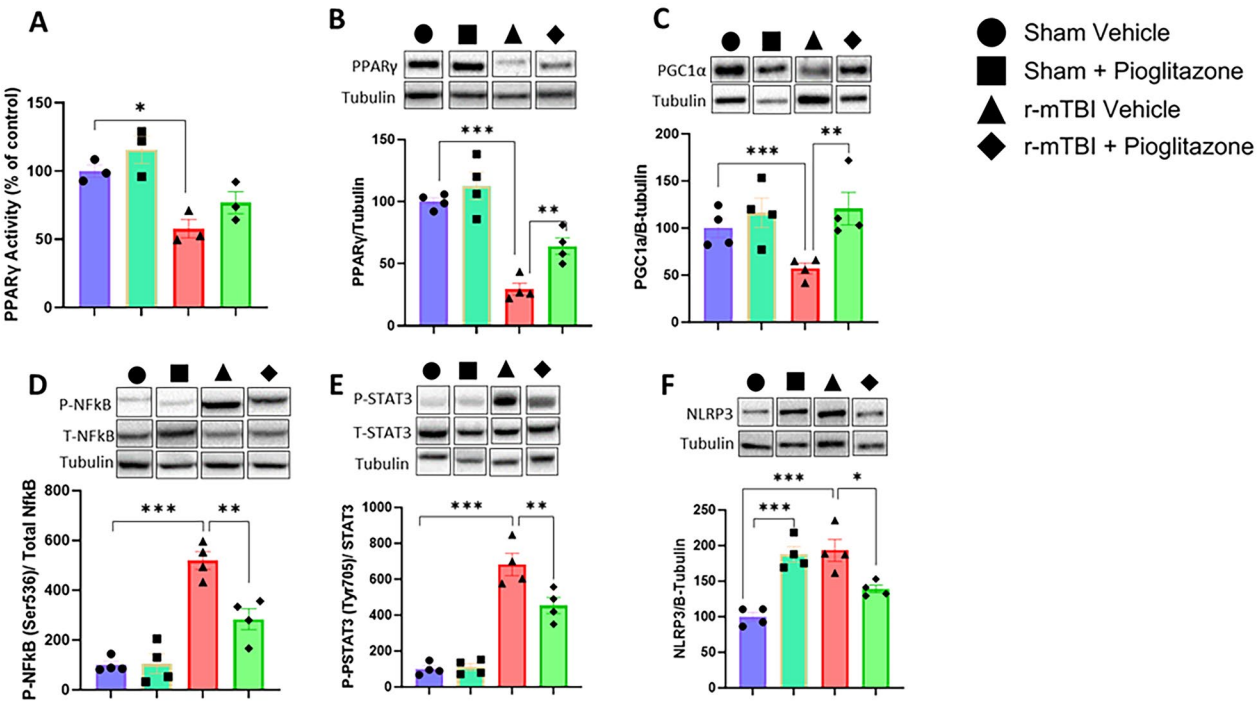

Fig. 7 Pioglitazone treatment rescues microglial PPARγ signaling and reduces inflammatory signaling. **A** Quantitation of PPARγ transcriptional activity in isolated microglia. Quantitation and representative immunoblots of PPARγ (**B**), PGC1α (**C**), Phospho NFκB (Ser536) (**D**), Phospho STAT3 (Tyr705) (**E**), and NLRP3 (**F**) in microglia isolated at six months post last injury from sham and injured mice who received Pioglitazone or vehicle treatment (n = 4/group). (**B**) (n = 3/group). Data were analyzed using a two-way ANOVA followed by Tukey's correction for multiple comparisons. All data are expressed as mean ± SEM percentage of control

Pioglitazone treatment reduces chronic microglial pro-inflammatory signaling

After demonstrating in vivo target engagement, we sought to assess how PPARγ agonism influences the microglial inflammatory signaling cascades in the aftermath of r-mTBI. As such we assessed the expression and activation of the pro-inflammatory transcription factors NFκB and STAT3. Both NFκB and STAT3 are well-acknowledged pro-inflammatory mediators and have been heavily implicated in the pathogenesis of neurodegenerative disorders [16, 55, 74, 119].

NFκB is a central component of the inflammatory cascade, as an early response transcription factor the activation of NFkB is regulated by phosphorylation and does not require the synthesis of new proteins enabling its immediate response to injury. As such, we assessed NFκB phosphorylation (Serine 536) to determine the effect of Pioglitazone treatment on the activation of NFκB signaling in isolated microglia (Fig. 7D). In line with our in vitro evidence, NFκB phosphorylation was significantly increased in microglia isolated from vehicle-treated r-mTBI mice compared to sham vehicle mice. Notably, the injury-induced increase in NFκB phosphorylation was reduced in mice treated with pioglitazone compared to vehicle treated mice.

Several studies have previously implicated microglial STAT3 pathway activation with the initiation of several pro-inflammatory processes in the aftermath of experimental brain trauma. As such, we assessed the effect of PPARγ agonism on STAT3 pathway activation (Fig. 7E). We observed that exposure to r-mTBI induced a chronic increase in microglial STAT3 phosphorylation compared to sham mice. However, our data demonstrate that pioglitazone treatment was able to significantly reduce STAT3 phosphorylation compared to vehicle-treated r-mTBI mice.

In addition to upregulating the expression of pro-inflammatory cytokines such as IL-6, IFNγ, and TNFα, NFκB activation has received increasing attention as a pivotal step in the activation of to the nucleotide-binding domain and leucine-rich repeat (NLR) family pyrin domain-containing protein 3 (NLRP3) inflammasome [2, 67]. This multimeric protein complex is an important link in the production of interleukin 1β (IL-1β), a pro-inflammatory cytokine that has repeatedly been implicated in secondary neuronal injury and the development of cognitive impairment and neurological disorders [13, 98, 108]. NLRP3 expression was significantly increased in microglia isolated from mice exposed to r-mTBI relative to sham mice. However, NLRP3 expression was markedly inhibited in injured mice who received pioglitazone relative to injured mice who received vehicle treatment (Fig. 7F). However, we did note that NLRP3 expression was significantly increased amongst sham animals who received Pioglitazone relative to sham vehicle-treated controls.

Pioglitazone treatment reduces microglial pro-inflammatory cytokine expression

To further examine the effects of r-mTBI and pioglitazone treatment on the inflammatory response to r-mTBI, we measured the intracellular concentrations of the pro-inflammatory cytokines IL-6, and TNFα in microglia isolated from sham and injured mice using a multiplex cytokine array. In line with our previous findings, microglia isolated from the brains of injured vehicle-treated mice expressed significantly higher levels of IL-6 ($p=0.004$) (Fig. 8A), and TNFα ($p \leq 0.001$) (Fig. 8B) relative to sham vehicle-treated animals. Furthermore,

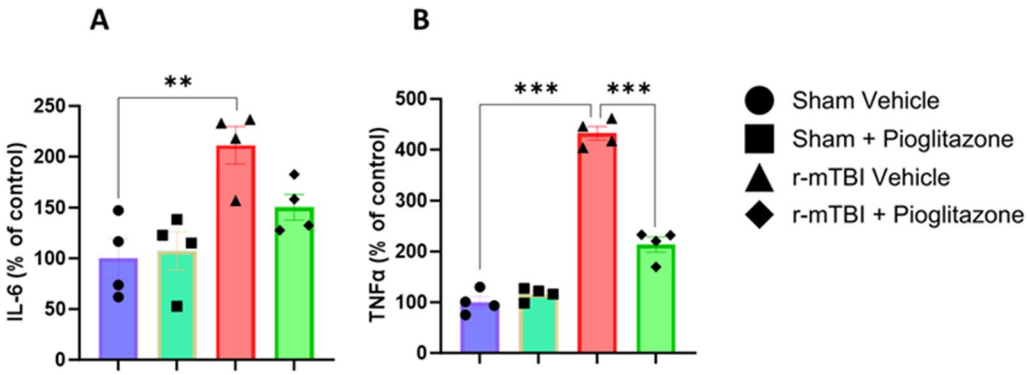

Fig. 8 PPARγ activation reduces chronic microglial pro-inflammatory cytokine production following exposure to r-mTBI. Microglia were isolated from sham and injured mice who received Pioglitazone (50ppm chow) or vehicle treatment and the concentrations of IL-6 (**A**) and TNFα (**B**) in cell lysates were assessed using the MSD multiplex cytokine array (n = 4/group). Data were analyzed using a two-way ANOVA followed by Tukey's correction for multiple comparisons. All data are expressed as mean ± SEM percentage of control

post-hoc analysis indicated that the injury-induced increase in TNFα was significantly blunted in injured mice who received Pioglitazone treatment relative to vehicle treated animals. However, Pioglitazone treatment in injured mice had no effect on IL-6 expression relative to injured mice who received vehicle treatment ($p = 0.158$).

Generation of a mouse model of microglial specific PPARγ overexpression

Our results demonstrate that delayed Pioglitazone treatment is effective in ameliorating the chronic microglial activation associated with exposure to r-mTBI. However, the broad expression of PPARγ by multiple CNS cell types [130], and the off-target effects of pharmacological PPARγ agonists make it difficult to disentangle the microglial specific effects of PPARγ activation to r-mTBI outcomes [136]. As such, we generated a microglial-specific tamoxifen-inducible mouse model of PPARγ activation by crossing the VP16-PPARγ LoxP mouse line with the CX3CR1-Cre recombinase mouse line (Fig. 9A, B). In this model, the constitutive overexpression and activation of PPARγ in CX3CR1-expressing cells is driven by the CAG-VP16 cytomegalovirus (CMV) immediate early enhancer/ chicken β-actin (CAG) promoter. Tamoxifen administration enables the translocation of CreER recombinase to the nucleus where it excises the floxed stop sequence. With the stop cassette removed, the PPARγ gene is now under the control of the CAG promoter. The CAG promoter is a strong, constitutive promoter composed of the CMV enhancer element, the chicken β-actin promoter, and the rabbit β-globin splice acceptor site, which induces high levels of gene expression. Furthermore, the VP16 sequence fused to PPARγ is a transcriptional activation domain derived from the herpes simplex virus that enhances the transcriptional activity of PPARγ. This activation is ligand-independent and results in a more potent and constant activation, bypassing the regulatory control of PPARγ activation exerted by ligand binding and co-factor interactions.

To validate the model, 8-week-old mcgPPARγ^{OE} mice were treated with tamoxifen or vehicle for 5 days. At 28 days post-last treatment, mice were euthanized and CD11b^{+ve} microglia were isolated and PPARγ expression and transcriptional activity was assessed (Fig. 9C, D). We observed a significant increase in the protein expression

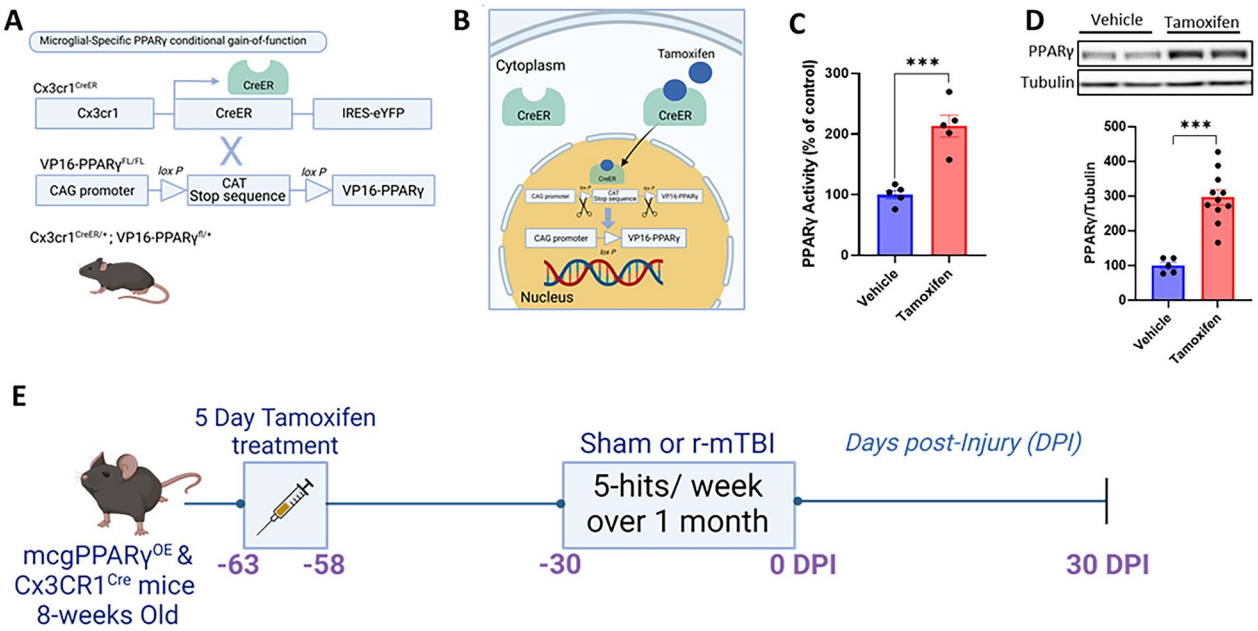

Fig. 9 Generation of a tamoxifen inducible microglial-specific PPARγ overexpression mouse line. **A**, **B** Graphic showing the generation of conditional PPARγ overexpressing mice and how tamoxifen treatment induces cre recombination in mcgPPARγ^{OE} mice. **C** To validate that tamoxifen treatment was able to induce cre-recombination, non-injured mcgPPARγ^{OE} mice received Tamoxifen (50mg/kg) or vehicle treatment for 5 days and the transcriptional activity of PPARγ in isolated microglia was assessed. **D** Quantitation and representative immunoblot of PPARγ expression in microglia isolated from vehicle and Tamoxifen treated mice ($n = 5–11$/group) **E** Graphic showing the experimental schedule. After validating that our treatment paradigm was sufficient to induce microglial PPARγ overexpression, 8 week old mcgPPARγ^{OE} and CX3CR1$^{CreERt2+/+}$ (Cre) mice received Tamoxifen for 5 days. At 12 weeks old, mice were exposed to our 20-hit r-mTBI paradigm or sham procedure. At 30 days post last injury all mice were euthanised and the brain tissue was processed for histopathology or microglia were isolated from the brain tissue for RNA sequencing

and transcriptional activity of PPARγ in microglia isolated from mice treated with tamoxifen compared to controls. Following validation of the mouse model, we sought to investigate how microglial-specific PPARγ overexpression influenced the microglial response to r-mTBI. PPARγ^{OE} and Cre-littermate mice were treated with tamoxifen at 8 weeks old for one week, then allowed 3 weeks for peripheral monocyte turnover. Mice were exposed to our 20-hit paradigm at 12 weeks old and then we assessed the microglial phenotype at 1 month post last injury by path and microglial RNA sequencing (Fig. 9E).

Microglial-specific PPARγ overexpression rescues chronic reactive gliosis

To assess the effect of microglial-specific PPARγ overexpression on the response to r-mTBI we assessed Iba1 and CD68 immunoreactivity. In accordance with our findings from wild type mice, we observed that exposure to r-mTBI increased Iba1, CD68, and GFAP immunoreactivity in the cortex, hippocampus and corpus callosum regardless of genotype. However, injured mcgPPARγ^{OE} mice exhibited significant reductions in Iba1, CD68, and GFAP immunoreactivity compared to injured CX3CR1$^{CreERt2+/+}$ controls in all areas assessed (Figs. 10, 11, 12A–O).

Microglial-specific PPARγ overexpression ameliorates the pro-inflammatory phenotype in response to r-mTBI

To further investigate the effect of mcgPPARγ^{OE} on the microglial phenotype following r-mTBI we performed unbiased RNA-sequencing on microglia isolated from both Injured and sham mcgPPARγ^{OE} mice and CX3CR1$^{CreERt2+/+}$ littermates at one month post last-injury.

We firstly analysed the effect of r-mTBI on the CX3CR1$^{CreERt2+/+}$ mice to establish a baseline effect of injury on the microglial phenotype (Fig. 13A, B). Differential expression analysis identified 1078 (708 Up, 370 Dn) differentially expressed genes (DEGs) in microglia isolated from Cre TBI and Cre sham mice. Exposure to r-mTBI induced the upregulation of several genes commonly observed in disease associated microglia (DAM) (Itgax, Cst7, Lpl, Clec7a, Hif1a, ApoE, Spp1) [14, 22, 62]. To better understand the altered signaling pathways and biological functions of microglia isolated from injured mice we performed gene enrichment and pathway analysis using IPA. Enrichment analysis revealed the significant upregulation of genes associated with Cytokine signaling, phagosome formation, and inflammasome pathway activation. Furthermore, we observed the downregulation of biological pathways associated with LXR/RXR, TGF-b, and AMPK signaling.

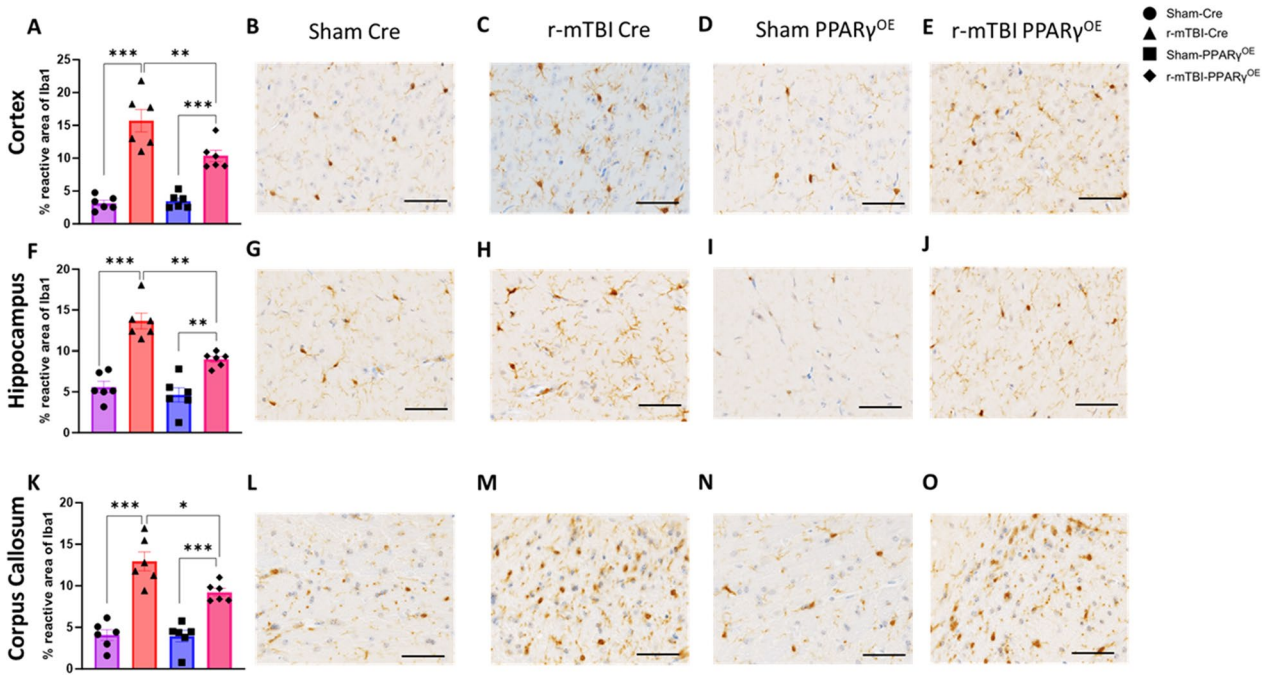

Fig. 10 Microglial-specific PPARγ overexpression reduces microglial Iba1 immunoreactivity at one month post r-mTBI. Quantitation and representative microscope images of Iba1^{+ve} immunoreactive area in the cortex (**A**–**E**), hippocampus (**F**–**J**), and Corpus Callosum (**K**–**O**) of mcg-PPARγ^{OE} and CX3CR1$^{CreERt2+/+}$ (Cre) (n = 6 per group). Data were analyzed using a two-way ANOVA followed by Tukey's correction for multiple comparisons. All data are expressed as mean ± SEM percentage reactive area

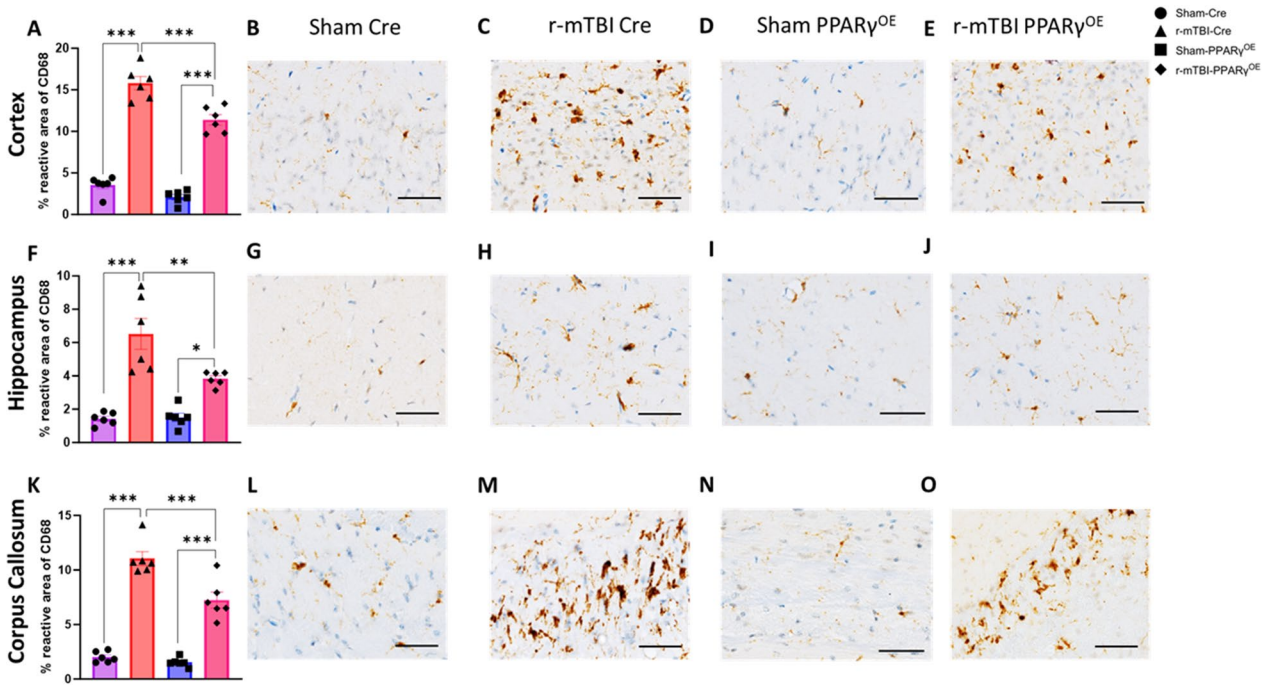

Fig. 11 Microglial-specific PPARγ overexpression reduces microglial CD68 immunoreactivity at one month post r-mTBI. Quantitation and representative microscope images of CD68^{+ve} immunoreactive area in the cortex (**A**–**E**), hippocampus (**F**–**J**), and Corpus Callosum (**K**–**O**) of mcg-PPARγ^{OE} and CX3CR1$^{CreERt2+/+}$ (Cre) (n = 6 per group). Data were analyzed using a two-way ANOVA followed by Tukey's correction for multiple comparisons. All data are expressed as mean ± SEM percentage reactive area

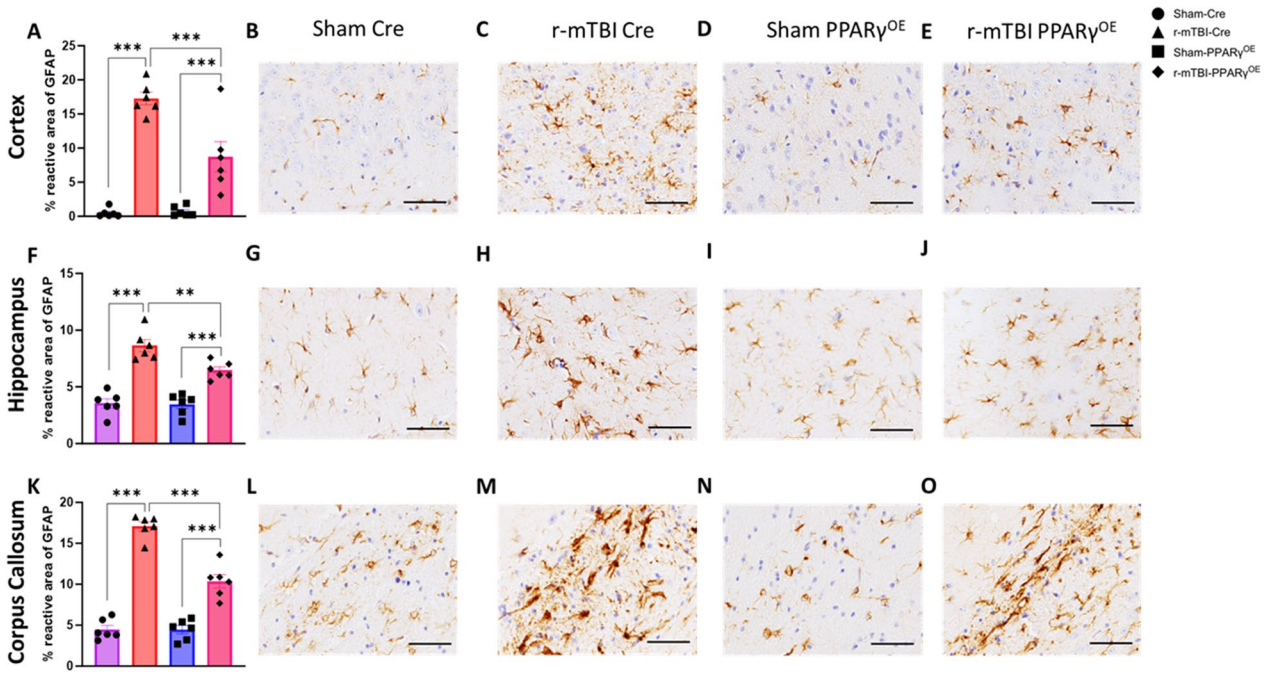

Fig. 12 Microglial-specific PPARγ overexpression reduces astrocyte GFAP immunoreactivity at one month post r-mTBI. Quantitation and representative microscope images of GFAP^{+ve} immunoreactive area in the cortex (**A**–**E**), hippocampus (**F**–**J**), and Corpus Callosum (**K**–**O**) of mcg-PPARγ^{OE} and CX3CR1$^{CreERt2+/+}$ (Cre) (n = 6 per group). Data were analyzed using a two-way ANOVA followed by Tukey's correction for multiple comparisons. All data are expressed as mean ± SEM percentage reactive area

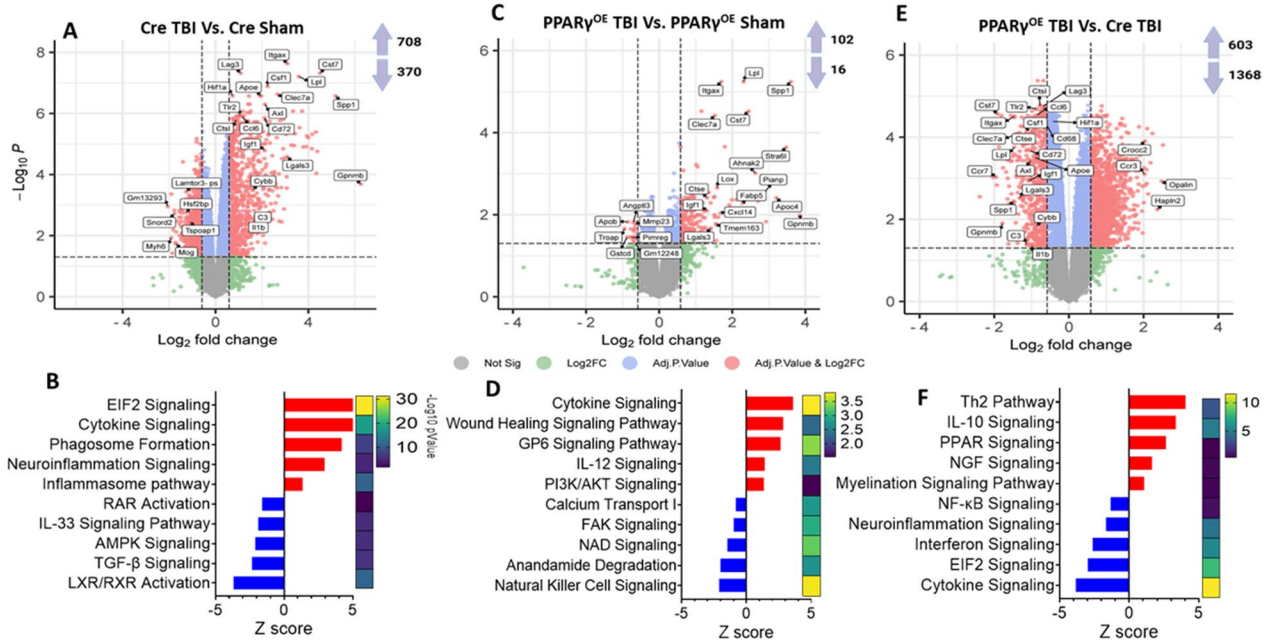

Fig. 13 PPARγ overexpression modifies the microglial response to r-mTBI. Volcano plots of injury-induced differential gene expression and histograms showing IPA gene enrichment of altered biological pathways in isolated microglia between injured and sham CX3CR1$^{CreERt2+/+}$- VP16-PPARγ$^{WT/WT}$ (Cre) mice (**A**, **B**), injured and sham mcgPPARγ^{OE} mice (**C**, **D**), and injured mcgPPARγ^{OE} vs injured CX3CR1$^{CreERt2+/+}$ mice (**E**, **F**), respectively (n = 4–5/group). Histograms show activation and inhibition of biological pathways by Z-score, corresponding heatmaps show the significance of pathway enrichement as − Log_{10} pValue

We next analysed the effect of r-mTBI exposure on microglia transcriptomic phenotype in mcgPPARγ^{OE} mice (Fig. 13C, D). Differential expression analysis identified only 118 (112Up, 16Dn) differentially expressed genes between injured and sham mice (approximately tenfold less DEG's than TBI vs sham CX3CR1$^{CreERt2+/+}$ mice). However, analysis of these differentially expressed genes revealed that injured mcgPPARγ^{OE} mice still exhibited a marked increase in some inflammatory and DAM genes (Lpl, Itgax, Spp1, Cst7, ApoE, Clec7a). This inflammatory response was also identified following gene enrichment analysis with cytokine signaling and IL-12 signaling pathways being significantly upregulated. Downregulated biological pathways between microglia isolated from injured and sham mcgPPARγ^{OE} mice included NAD signaling, FAK signaling, and Anandamide signaling.

We then compared the transcriptome of microglia isolated from injured mcgPPARγ^{OE} and CX3CR1$^{CreERt2+/+}$ mice to examine how PPARγ^{OE} influences the inflammatory response in the chronic aftermath of r-mTBI (Fig. 13E, F). Differential expression analysis identified 1971 DEGs (603Up, 1368Dn). Top upregulated genes in injured PPARγ^{OE} mice included Gprasp2, Plcg1, Ide, Cfap141, and Ccr5. Downregulated genes included Cstc, Siglecf, Tlr2, Cstl, and Rpl19. Gene enrichment analysis revealed that injured PPARγ^{OE} mice exhibited an upregulation of genes associated with reparative pathways, such as IL-10 signaling, PPARγ signaling, and myelination signaling pathways and a downregulation of genes associated with Cytokine signaling, Neuroinflammation, and EIF2 signaling.

Microglial-specific PPARγ overexpression reduces pro-inflammatory, and Disease associated microglia Gene expression

To assess how the microglial responses to r-mTBI and PPARγ overexpression relate to other neurological diseases, we used a hypothesis driven approach to compare the microglial transcriptomes from sham and injured mcgPPARγ^{OE} and CX3CR1$^{CreERt2+/+}$ mice against the gene signature of DAM microglia seen in certain neurodegenerative disorders (Fig. 14). We observed that exposure to r-mTBI results in the increased expression of several DAM genes and the downregulation of homeostatic genes. Notably, mcgPPARγ^{OE} was able to prevent this transition towards a "DAM-like" state suggesting a neuroprotective phenotype.

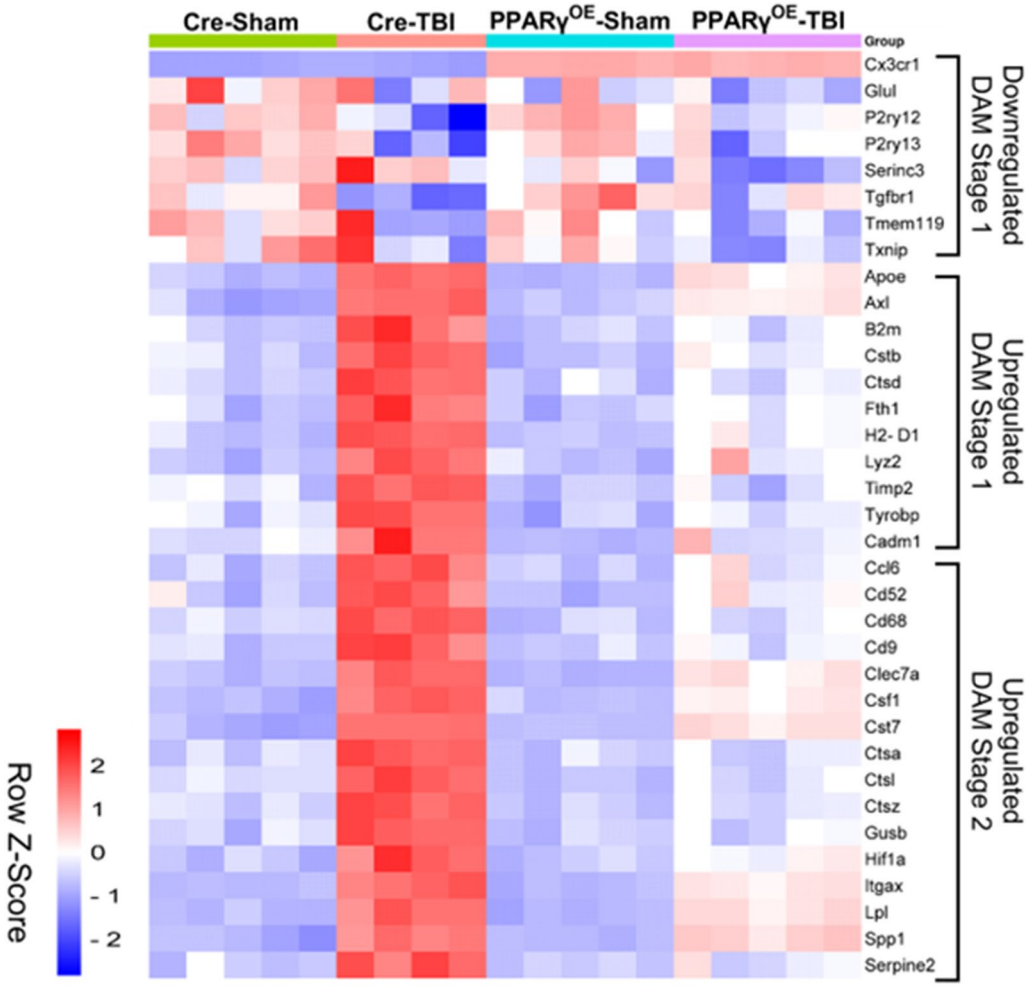

Fig. 14 Microglial PPARγ overexpression prevents the adoption of a disease associated microglia-like (DAM-like) phenotype at 30 days post r-mTBI. Heatmap depicting the expression of DAM genes (rows) across CX3CR1$^{CreERt2+/+}$ (Cre) and mcgPPARγ^{OE} mice (n = 4–5/group) who received r-mTBI or sham procedures (columns). Data are expressed as row z-score (red corresponds to gene upregulation and blue to downregulation)

Discussion

Chronic neuroinflammation and microglial activation are hallmark features of traumatic brain injury [44, 64, 117, 134]. However, the underlying mechanisms driving microglial pathobiology in the chronic aftermath of r-mTBI remain unclear [77]. PPARγ is a nuclear transcription factor that is well expressed in immune cells such as microglia [9, 10, 121]. As a nuclear transcription factor, PPARγ signaling has been implicated in several cellular functions, including lipid and glucose metabolism, cell proliferation, and inflammation [12, 35, 80, 112, 115, 129]. While several studies have investigated the potential of PPARγ agonism to beneficially influence the pathogenic cascades that mediate secondary tissue damage following brain trauma [24, 49, 53, 137, 139, 142], dissecting the microglial specific effects of PPARγ agonism has thus far been difficult to achieve in vivo. Therefore, in the present study, we utilized both pharmacological studies and a conditional transgenic mouse overexpressing PPARγ in microglia to investigate the beneficial effects of PPARγ agonism on microglial pathobiology in the aftermath of r-mTBI. We demonstrated that activation of PPARγ reduces microglial inflammatory pathway activation and inhibits pro-inflammatory cytokine production. Furthermore, we also present evidence to demonstrate the delayed Pioglitazone treatment can ameliorate r-mTBI neuropathology and cognitive impairment.

In the present study we found that exposure to r-mTBI or the pro-inflammatory stimuli LPS inhibited the expression and activity of PPARγ in microglia. While a similar decrease in PPARγ expression and activity has been observed in several studies of CNS and peripheral

inflammation [15, 43, 45, 79, 95, 125, 132], the exact mechanism driving the downregulation of PPARγ expression and activity in response to inflammatory stimuli is still unclear. Furthermore, while the true cause of this downregulation is likely disease specific, Shibuya and colleagues proposed that the increased production of superoxide and Nitric oxide (NO) radicals in response to LPS, TNFα, or peroxynitrite exposure results in the nitration of PPARγ tyrosine residues, preventing ligand interaction and subsequent nuclear translocation. Furthermore, the authors noted that due to the central roles of PPARγ in inflammation and immune responses, the suppression of PPARγ activity by ROS might promote chronic or recurrent inflammation [114]. Together these data support the hypothesis that impaired PPARγ signaling in microglia is a critical driver of chronic dysregulated microglial activation and therefore represents a promising therapeutic target to ameliorate CNS inflammation and improve r-mTBI outcomes.

Cognitive and functional impairments are amongst the most commonly reported clinical symptoms of TBI [26, 113]. The remediation of these learning and memory deficits remains a major aspiration of both clinical and preclinical TBI researchers. However, no therapeutic interventions have thus far demonstrated substantial efficacy [36, 66, 120]. Our laboratory has previously developed several preclinical models of repetitive brain trauma using closed head mid-line impact model of r-mTBI using the same impact parameters but varying the quantity and chronicity of impacts [28, 29, 81, 83–86, 94, 96, 100]. Consistent with our previous work, here we demonstrated that exposure to our 20-hit r-mTBI paradigm induces chronic spatial learning and memory deficits. We observed that Pioglitazone treatment markedly improved performance in both the acquisition and probe phases of the Barnes maze. These results are in line with the work of several others who have reported improved cognitive performance in preclinical models of CNS trauma, neurodegeneration, and aging in response to PPARγ agonist treatment [20, 89, 101, 128]. The close link between diabetes and the development of cognitive decline has led many researchers to investigate how Pioglitazone may prevent cognitive dysfunction. While the complete mechanisms underlying the neuroprotective activity of Pioglitazone have not yet been fully elucidated, multiple studies have shown that pioglitazone treatment increased short- and long-term memory through the preservation of synaptic plasticity and integrity [18, 111]. Some studies have suggested that the neuroprotective effect of Pioglitazone is mediated through its ability to prevent the mis-sorting and hyperphosphorylation of tau via the inhibition of CDK5 [79]. While tau pathology is highly relevant to TBI and is considered a pathognomic feature of neurodegenerative disorders such as chronic traumatic encephalopathy (CTE), previous studies of r-mTBI from our laboratory have shown little evidence of tau pathology out to one-year post-injury in wild-type mice suggesting that the development of toxic tau species is likely not a driving factor of the cognitive impairment seen in this study [83].

In both our protein and transcriptome analysis of isolated microglia we observed that microglial PPARγ agonism reduces chronic pro-inflammatory activation following r-mTBI via the suppression of NFκB signaling. In the CNS, NFkB signaling has been implicated in regulating several physiological and pathological processes. Under baseline conditions, NFkB resides in the cytoplasm in a complex with inhibitory IkB proteins [41, 42]. However, following stimulation by DAMPs, cytokines, or oxidative stress NFkB rapidly becomes activated and is translocated to the nucleus, where it initiates transcriptional programs which mediate the expression of several inflammatory genes [61]. NFkB is thought to be critical in the propagation of inflammatory responses, as many of the NFkB-induced gene expression products act on receptors that, in turn, also activate NFkB. This feed forward mechanism of NFkB is thought to be a major mediator of the chronic inflammation that follows TBI [92]. PPARγ agonism has been shown to inhibit NFkB through several potential mechanisms. In addition to the inhibition of NFkB via direct binding, PPARγ agonism has been shown to suppress NFkB pathway signaling through IL-4 and IL-10 signaling [56, 106, 127]. This finding agrees with our transcriptomic analysis of mcgPPARγ^{OE} mice which found that PPAR activation increased IL-10 signaling suggesting a potential neuroprotective mechanism for the observed improvements in cognitive and neuropathological outcomes.

While NFkB has long been acknowledged as a central molecule in inflammation following TBI [92], the contributions of the NLRP3 inflammasome, or the adoption of a DAM-like phenotype to TBI pathobiology, and importantly, their regulation by PPARγ have only recently become acknowledged and are still under investigation [50, 117, 138]. NLRs are cytosolic pattern recognition receptors that, when activated, form the inflammasome complex, and mediate the production of IL-1β and IL-18 through caspase-1 processing [52, 122]. While these interleukins do play critical roles in normal wound healing, they have been shown to promote the accumulation of reactive oxygen and nitrogen species [5, 75, 118]. This feed-forward mechanism of oxidative damage and inflammasome activation has been suggested to promote inflammatory neuronal cell death, known as pyroptosis, and is commonly seen in neurodegenerative disorders [39, 40, 48]. Studies of both TBI and spinal cord injury

have shown that PPARγ agonism was able to inhibit the NLRP3 mediated production of IL-1β through the inhibition of caspase-1, with these studies noting that reduced NLRP3 activity was strongly correlated with improved functional and pathological outcomes [76, 138]. Together, the intricate interplay between PPARγ, NFκB, and inflammasome signaling underscores the complexity of neuroinflammatory mechanisms and the potential of PPARγ modulation as a multifaceted therapeutic strategy.

In the present study, Tamoxifen treatment was administered before animals were exposed to our 20-hit r-mTBI paradigm. While this prophylactic treatment paradigm demonstrated effective target engagement and has been used in several other studies to investigate the mechanisms of experimental brain injury [33, 135, 141], it is possible that the effects we observed in this study may have been even more pronounced if Tamoxifen treatment was administered after exposure to experimental brain injury. In addition to the increased clinical relevance of a post-injury treatment paradigm, following exposure to r-mTBI microglia rapidly proliferate and migrate towards the injury site [25, 77, 133]. These "new-born" microglia which have not been exposed to Tamoxifen will not have undergone Cre recombination and therefore will not express constitutively active PPARγ, potentially limiting our analysis of the therapeutic efficacy of microglial PPARγ overexpression. Therefore, future studies should carefully consider the timing of gene recombination when designing such studies.

It has to be acknowledged that in the present study we did observe some negative side effects in sham animals treated with Pioglitazone. Specifically, we observed that some sham animals treated with Pioglitazone exhibited an increase in the microglial expression of NLRP3. While the mechanism driving this phenomenon requires further investigation, the clinical use of Pioglitazone is associated with multiple complications including weight gain, fluid retention, congestive heart failure, and accelerated bone loss [90]. The associated side effects and poor pharmacokinetic profile of earlier generation thiazolidinediones such as Pioglitazone and Rosiglitazone limit their potential clinical utility. However, later generation PPARγ agonists such as the recently developed Leriglitazone may have the potential to reduce the side effects associated with Pioglitazone. Leriglitazone is a novel active metabolite of Pioglitazone which has been shown to promote neuroprotection in both neurons and astrocytes, improves axon myelination, and preserves BBB integrity in models of adrenoleukodystrophy [87]. Furthermore, pharmacokinetic and pharmacodynamic studies have demonstrated that Leriglitazone has a greater ability to cross the BBB [109], and better transcriptional efficacy than Pioglitazone [82]. Together, these factors mean that lower doses of Leriglitazone could be able to ameliorate the chronic deleterious sequelae of r-mTBI while minimizing any potential negative side effects. Leriglitazone is currently being evaluated for the treatment of cerebral adrenoleukodystrophy [109], adrenomyeloneuropathy [60], and Friedreich's ataxia [99]. These conditions all share a neuroinflammatory aspect which shows overlap with TBI [4, 131, 140]. As such, the investigation of Leriglitazone in r-mTBI may hold strong clinical utility for the treatment of traumatic brain injury.

In conclusion, our results highlight the potential of Pioglitazone and microglial-specific PPARγ overexpression as promising strategies to modulate neuroinflammation and improve cognitive outcomes following r-mTBI. It is particularly noteworthy that Pioglitazone's effects were not limited to the acute phase but extended to chronic phases of r-mTBI, suggesting that there is a prolonged timeframe in which treatment can elicit therapeutic benefits. The microglial-specific PPARγ overexpression model reinforced these findings, emphasizing the importance of targeting microglial-specific pathways for long-term neuroprotection. While this study provides promising insights, further investigations are warranted to elucidate the precise molecular mechanisms underlying PPARγ-mediated neuroprotection. As such, the development of mcgPPARγ^{OE} mice in this study provides a valuable platform to interrogate the microglial-specific therapeutic mechanisms of not only PPARγ activation but also the activation of its downstream cellular mediators. Additionally, clinical translation of these findings may hold significant implications for developing novel therapeutic interventions for individuals with a history of repeated brain injuries.

Acknowledgements
Dr. Crawford is a Research Career Scientist at the James A. Haley Veterans Hospital, Tampa, FL. We would like to thank the Roskamp Institute for their generosity in helping to make this work possible.

Author contributions
Conceptualization: AP, MM, FC, and JO. Methodology: AP, FC, and JO. Investigation, AP, MK, ME, CO, MB, TV, and JO. Data analysis: AP, CT, ME, and JO. Resources: MM, FC, and JO. Writing—original draft, AP and JO. Writing—review and editing: AP, ME, FC, and JO. Supervision: MM, FC, and JO. Funding acquisition: FC and JO.

Funding
This work was supported by the National Institute of Health (NIH) under award number 5R03AG075365-02 and by the U.S. Department of Defense under award number W81XWH-17-1-0638 to FC and JO. Opinions, interpretations, conclusions, and recommendations are those of the author and are not necessarily endorsed by the National Institute of Health.

Availability of data and materials
The raw data that support the findings of this study are available upon reasonable request to the corresponding author.

Declarations

Ethics approval and consent to participate

The current study does not involve human participants, human tissue, or data. All animal experiments were reviewed and approved by the Institutional Animal Care and Use Committee (IACUC) at the Roskamp Institute (Protocol #R092). All procedures were performed in accordance with IACUC and the NIH Guidelines for the Care and Use of Laboratory Animals.

Competing interests

The authors declare they have no competing interests.

Received: 15 February 2024 Accepted: 12 July 2024
Published online: 03 August 2024

References

1. Afgan E, Baker D, Batut B, van den Beek M, Bouvier D, Čech M, Chilton J, Clements D, Coraor N, Grüning BA, Guerler A, Hillman-Jackson J, Hiltemann S, Jalili V, Rasche H, Soranzo N, Goecks J, Taylor J, Nekrutenko A, Blankenberg D. The Galaxy platform for accessible, reproducible and collaborative biomedical analyses: 2018 update. Nucleic Acids Res. 2018;46(W1):W537–44. https://doi.org/10.1093/nar/gky379.
2. Afonina IS, Zhong Z, Karin M, Beyaert R. Limiting inflammation—the negative regulation of NF-κB and the NLRP3 inflammasome. Nat Immunol. 2017;18(8):861–9. https://doi.org/10.1038/ni.3772.
3. Andrews S. FastQC: A quality control tool for High-Throughput sequence data. 2010. http://www.bioinformatics.babraham.ac.uk/Projects/Fastqc/. Accessed 19 Nov 2023.
4. Apolloni S, Milani M, D'Ambrosi N. Neuroinflammation in Friedreich's ataxia. Int J Mol Sci. 2022;23(11):6297. https://doi.org/10.3390/ijms23116297.
5. Bai H, Yang B, Yu W, Xiao Y, Yu D, Zhang Q. Cathepsin B links oxidative stress to the activation of NLRP3 inflammasome. Exp Cell Res. 2018;362(1):180–7. https://doi.org/10.1016/j.yexcr.2017.11.015.
6. Bailes JE, Dashnaw ML, Petraglia AL, Turner RC. Cumulative effects of repetitive mild traumatic brain injury. Concussion. 2014. https://doi.org/10.1159/000358765.
7. Bauer ME, Teixeira AL. Neuroinflammation in mood disorders: role of regulatory immune cells. NeuroImmunoModulation. 2021;28(3):99–107. https://doi.org/10.1159/000515594.
8. Baugh CM, Robbins CA, Stern RA, McKee AC. Current understanding of chronic traumatic encephalopathy. Curr Treat Options Neurol. 2014;16(9):306. https://doi.org/10.1007/s11940-014-0306-5.
9. Bernardo A, Minghetti L. PPAR-γ agonists as regulators of microglial activation and brain inflammation. Curr Pharm Design. 2006;12(1):93–109. https://doi.org/10.2174/138161206780574579.
10. Bernardo A, Minghetti L. Regulation of glial cell functions by PPAR-natural and synthetic agonists. PPAR Res. 2008;2008:1–10. https://doi.org/10.1155/2008/864140.
11. Bolger AM, Lohse M, Usadel B. Trimmomatic: a flexible trimmer for Illumina sequence data. Bioinformatics. 2014;30(15):2114–20. https://doi.org/10.1093/bioinformatics/btu170.
12. Bright JJ, Kanakasabai S, Chearwae W, Chakraborty S. PPAR regulation of inflammatory signaling in CNS diseases. PPAR Res. 2008;2008:1–12. https://doi.org/10.1155/2008/658520.
13. Burm SM, Peferoen LAN, Zuiderwijk-Sick EA, Haanstra KG, t' Hart BA, van der Valk P, Amor S, Bauer J, Bajramovic JJ. Expression of IL-1β in rhesus EAE and MS lesions is mainly induced in the CNS itself. J Neuroinflammation. 2016;13(1):138. https://doi.org/10.1186/s12974-016-0605-8.
14. Butovsky O, Weiner HL. Microglial signatures and their role in health and disease. Nat Rev Neurosci. 2018;19(10):622–35. https://doi.org/10.1038/s41583-018-0057-5.
15. Cai W, Yang T, Liu H, Han L, Zhang K, Hu X, Zhang X, Yin K-J, Gao Y, Bennett MVL, Leak RK, Chen J. Peroxisome proliferator-activated receptor γ (PPARγ): a master gatekeeper in CNS injury and repair. Prog Neurobiol. 2018;163–164:27–58. https://doi.org/10.1016/j.pneurobio.2017.10.002.
16. Chen E, Xu D, Lan X, Jia B, Sun L, Zheng J, Peng H. A novel role of the STAT3 pathway in brain inflammation-induced human neural progenitor cell differentiation. Curr Mol Med. 2013;13(9):1474–84. https://doi.org/10.2174/15665240113139990076.
17. Chen F, Wang M, O'Connor JP, He M, Tripathi T, Harrison LE. Phosphorylation of PPAR? via active ERK1/2 leads to its physical association with p65 and inhibition of NF-?? J Cell Biochem. 2003;90(4):732–44. https://doi.org/10.1002/jcb.10668.
18. Chen J, Li S, Sun W, Li J. Anti-diabetes drug pioglitazone ameliorates synaptic defects in AD transgenic mice by inhibiting cyclin-dependent kinase 5 activity. PLoS ONE. 2015;10(4): e0123864. https://doi.org/10.1371/journal.pone.0123864.
19. Collins MW, Lovell MR, Iverson GL, Cantu RC, Maroon JC, Field M. Cumulative effects of concussion in high school athletes. Neurosurgery. 2002;51(5):1175–81. https://doi.org/10.1097/00006123-200211000-00011.
20. Cowley TR, O'Sullivan J, Blau C, Deighan BF, Jones R, Kerskens C, Richardson JC, Virley D, Upton N, Lynch MA. Rosiglitazone attenuates the age-related changes in astrocytosis and the deficit in LTP. Neurobiol Aging. 2012;33(1):162–75. https://doi.org/10.1016/j.neurobiolaging.2010.02.002.
21. Dean PJA, Sterr A. Long-term effects of mild traumatic brain injury on cognitive performance. Front Hum Neurosci. 2013. https://doi.org/10.3389/fnhum.2013.00030.
22. Deczkowska A, Keren-Shaul H, Weiner A, Colonna M, Schwartz M, Amit I. Disease-associated microglia: a universal immune sensor of neurodegeneration. Cell. 2018;173(5):1073–81. https://doi.org/10.1016/j.cell.2018.05.003.
23. Delaney JS, Lacroix VJ, Gagne C, Antoniou J. Concussions among university football and soccer players: a pilot study. Clin J Sport Med. 2001;11(4):234–40. https://doi.org/10.1097/00042752-200110000-00005.
24. Deng Y, Jiang X, Deng X, Chen H, Xu J, Zhang Z, Liu G, Yong Z, Yuan C, Sun X, Wang C. Pioglitazone ameliorates neuronal damage after traumatic brain injury via the PPARγ/NF-κB/IL-6 signaling pathway. Genes Dis. 2020. https://doi.org/10.1016/j.gendis.2019.05.002.
25. Donat CK, Scott G, Gentleman SM, Sastre M. Microglial activation in traumatic brain injury. Front Aging Neurosci. 2017. https://doi.org/10.3389/fnagi.2017.00208.
26. Dunning DL, Westgate B, Adlam A-LR. A meta-analysis of working memory impairments in survivors of moderate-to-severe traumatic brain injury. Neuropsychology. 2016;30(7):811–9. https://doi.org/10.1037/neu0000285.
27. Dunning M. AnnotateMyIDs · bio.tools. AnnotateMyIDs. 2017. https://bio.tools/annotatemyids
28. Eisenbaum M, Pearson A, Gratkowski A, Mouzon B, Mullan M, Crawford F, Ojo J, Bachmeier C. Influence of traumatic brain injury on extracellular tau elimination at the blood–brain barrier. Fluids Barriers CNS. 2021. https://doi.org/10.1186/s12987-021-00283-y.
29. Eisenbaum M, Pearson A, Ortiz C, Mullan M, Crawford F, Ojo J, Bachmeier C. ApoE4 expression disrupts tau uptake, trafficking, and clearance in astrocytes. Glia. 2024;72(1):184–205. https://doi.org/10.1002/glia.24469.
30. Ewels P, Magnusson M, Lundin S, Käller M. MultiQC: summarize analysis results for multiple tools and samples in a single report. Bioinformatics. 2016;32(19):3047–8. https://doi.org/10.1093/bioinformatics/btw354.
31. Ferguson SA, Mouzon BC, Lynch C, Lungmus C, Morin A, Crynen G, Carper B, Bieler G, Mufson EJ, Stewart W, Mullan M, Crawford F. Negative impact of female sex on outcomes from repetitive mild traumatic brain injury in hTau mice is age dependent: a chronic effects of neurotrauma consortium study. Front Aging Neurosci. 2017. https://doi.org/10.3389/fnagi.2017.00416.
32. Ferguson S, Mouzon B, Paris D, Aponte D, Abdullah L, Stewart W, Mullan M, Crawford F. Acute or delayed treatment with anatabine improves spatial memory and reduces pathological sequelae at late time-points after repetitive mild traumatic brain injury. J Neurotrauma. 2017. https://doi.org/10.1089/neu.2016.4636.
33. Fonseca MI, Chu S-H, Hernandez MX, Fang MJ, Modarresi L, Selvan P, MacGregor GR, Tenner AJ. Cell-specific deletion of C1qa identifies microglia as the dominant source of C1q in mouse brain. J Neuroinflammation. 2017;14(1):48. https://doi.org/10.1186/s12974-017-0814-9.

34. Fu R, Shen Q, Xu P, Luo JJ, Tang Y. Phagocytosis of microglia in the central nervous system diseases. Mol Neurobiol. 2014;49(3):1422–34. https://doi.org/10.1007/s12035-013-8620-6.
35. Gervois P, Torra IP, Fruchart J-C, Staels B. Regulation of lipid and lipoprotein metabolism by PPAR activators. Clin Chem Lab Med. 2000. https://doi.org/10.1515/CCLM.2000.002.
36. Graham NS, Sharp DJ. Understanding neurodegeneration after traumatic brain injury: from mechanisms to clinical trials in dementia. J Neurol Neurosurg Psychiatry. 2019;90(11):1221–33. https://doi.org/10.1136/jnnp-2017-317557.
37. Guergues J, Zhang P, Liu B, Stevens SM. Improved methodology for sensitive and rapid quantitative proteomic analysis of adult-derived mouse microglia: application to a novel in vitro mouse microglial cell model. Proteomics. 2019;19(11):1800469. https://doi.org/10.1002/pmic.201800469.
38. Guskiewicz KM, Marshall SW, Bailes J, McCrea M, Cantu RC, Randolph C, Jordan BD. Association between recurrent concussion and late-life cognitive impairment in retired professional football players. Neurosurgery. 2005;57(4):719–26. https://doi.org/10.1227/01.NEU.0000175725.75780.DD.
39. Hanslik KL, Ulland TK. The role of microglia and the Nlrp3 inflammasome in Alzheimer's disease. Front Neurol. 2020. https://doi.org/10.3389/fneur.2020.570711.
40. Harijith A, Ebenezer DL, Natarajan V. Reactive oxygen species at the crossroads of inflammasome and inflammation. Front Physiol. 2014. https://doi.org/10.3389/fphys.2014.00352.
41. Hayden MS, Ghosh S. Shared principles in NF-κB signaling. Cell. 2008;132(3):344–62. https://doi.org/10.1016/j.cell.2008.01.020.
42. Hayden MS, Ghosh S. NF-κB, the first quarter-century: remarkable progress and outstanding questions. Genes Dev. 2012;26(3):203–34. https://doi.org/10.1101/gad.183434.111.
43. Heming M, Gran S, Jauch S-L, Fischer-Riepe L, Russo A, Klotz L, Hermann S, Schäfers M, Roth J, Barczyk-Kahlert K. Peroxisome proliferator-activated receptor-γ modulates the response of macrophages to lipopolysaccharide and glucocorticoids. Front Immunol. 2018. https://doi.org/10.3389/fimmu.2018.00893.
44. Henry R, Loane D. Targeting chronic and evolving neuroinflammation following traumatic brain injury to improve long-term outcomes: insights from microglial-depletion models. Neural Regen Res. 2021;16(5):976. https://doi.org/10.4103/1673-5374.297068.
45. Hernandez-Quiles M, Broekema MF, Kalkhoven E. PPARgamma in metabolism, immunity, and cancer: unified and diverse mechanisms of action. Front Endocrinol. 2021. https://doi.org/10.3389/fendo.2021.624112.
46. Herrero Babiloni A, Baril A-A, Charlebois-Plante C, Jodoin M, Sanchez E, De Baets L, Arbour C, Lavigne GJ, Gosselin N, De Beaumont L. The putative role of neuroinflammation in the interaction between traumatic brain injuries, sleep, pain and other neuropsychiatric outcomes: a state-of-the-art review. J Clin Med. 2023;12(5):1793. https://doi.org/10.3390/jcm12051793.
47. Hopperton KE, Mohammad D, Trépanier MO, Giuliano V, Bazinet RP. Markers of microglia in post-mortem brain samples from patients with Alzheimer's disease: a systematic review. Mol Psychiatry. 2018;23(2):177–98. https://doi.org/10.1038/mp.2017.246.
48. Hu X, Chen H, Xu H, Wu Y, Wu C, Jia C, Li Y, Sheng S, Xu C, Xu H, Ni W, Zhou K. Role of pyroptosis in traumatic brain and spinal cord injuries. Int J Biol Sci. 2020;16(12):2042–50. https://doi.org/10.7150/ijbs.45467.
49. Hui Y, Zhao H, Shi L, Zhang H. Traumatic brain injury-mediated neuroinflammation and neurological deficits are improved by 8-methoxypsoralen through modulating PPARγ/NF-κB pathway. Neurochem Res. 2023;48(2):625–40. https://doi.org/10.1007/s11064-022-03788-6.
50. Irrera N, Russo M, Pallio G, Bitto A, Mannino F, Minutoli L, Altavilla D, Squadrito F. The role of NLRP3 inflammasome in the pathogenesis of traumatic brain injury. Int J Mol Sci. 2020;21(17):6204. https://doi.org/10.3390/ijms21176204.
51. Jarrahi A, Braun M, Ahluwalia M, Gupta RV, Wilson M, Munie S, Ahluwalia P, Vender JR, Vale FL, Dhandapani KM, Vaibhav K. Revisiting traumatic brain injury: from molecular mechanisms to therapeutic interventions. Biomedicines. 2020;8(10):389. https://doi.org/10.3390/biomedicines8100389.
52. Jha S, Srivastava SY, Brickey WJ, Iocca H, Toews A, Morrison JP, Chen VS, Gris D, Matsushima GK, Ting JP-Y. The inflammasome sensor, NLRP3, regulates CNS inflammation and demyelination via caspase-1 and interleukin-18. J Neurosci. 2010;30(47):15811–20. https://doi.org/10.1523/JNEUROSCI.4088-10.2010.
53. Jiang Q, Chen J, Long X, Yao X, Zou X, Yang Y, Huang G, Zhang H. Phillyrin protects mice from traumatic brain injury by inhibiting the inflammation of microglia via PPARγ signaling pathway. Int Immunopharmacol. 2020;79: 106083. https://doi.org/10.1016/j.intimp.2019.106083.
54. Johnson WD, Griswold DP. Traumatic brain injury: a global challenge. Lancet Neurol. 2017;16(12):949–50. https://doi.org/10.1016/S1474-4422(17)30362-9.
55. Kaltschmidt B, Helweg LP, Greiner JFW, Kaltschmidt C. NF-κB in neurodegenerative diseases: recent evidence from human genetics. Front Mol Neurosci. 2022. https://doi.org/10.3389/fnmol.2022.954541.
56. Kaltschmidt B, Widera D, Kaltschmidt C. Signaling via NF-κB in the nervous system. Biochim Biophys Acta BBA Mol Cell Res. 2005;1745(3):287–99. https://doi.org/10.1016/j.bbamcr.2005.05.009.
57. Kim D, Langmead B, Salzberg SL. HISAT: a fast spliced aligner with low memory requirements. Nat Methods. 2015;12(4):357–60. https://doi.org/10.1038/nmeth.3317.
58. Kim SM, McIlwraith EK, Chalmers JA, Belsham DD. Palmitate induces an anti-inflammatory response in immortalized microglial BV-2 and IMG cell lines that decreases TNFα levels in mHypoE-46 hypothalamic neurons in co-culture. Neuroendocrinology. 2018;107(4):387–99. https://doi.org/10.1159/000494759.
59. Kleinhenz JM, Murphy TC, Pokutta-Paskaleva AP, Gleason RL, Lyle AN, Taylor WR, Blount MA, Cheng J, Yang Q, Sutliff RL, Hart CM. Smooth muscle-targeted overexpression of peroxisome proliferator activated receptor-γ disrupts vascular wall structure and function. PLoS ONE. 2015;10(10): e0139756. https://doi.org/10.1371/journal.pone.0139756.
60. Köhler W, Engelen M, Eichler F, Lachmann R, Fatemi A, Sampson J, Salsano E, Gamez J, Molnar MJ, Pascual S, Rovira M, Vilà A, Pina G, Martín-Ugarte I, Mantilla A, Pizcueta P, Rodríguez-Pascau L, Traver E, Vilalta A, Hashmi S. Safety and efficacy of leriglitazone for preventing disease progression in men with adrenomyeloneuropathy (ADVANCE): a randomised, double-blind, multi-centre, placebo-controlled phase 2–3 trial. Lancet Neurol. 2023;22(2):127–36. https://doi.org/10.1016/S1474-4422(22)00495-1.
61. Kopitar-Jerala N. Innate immune response in brain, NF-kappa B signaling and cystatins. Front Mol Neurosci. 2015. https://doi.org/10.3389/fnmol.2015.00073.
62. Krasemann S, Madore C, Cialic R, Baufeld C, Calcagno N, El Fatimy R, Beckers L, O'Loughlin E, Xu Y, Fanek Z, Greco DJ, Smith ST, Tweet G, Humulock Z, Zrzavy T, Conde-Sanroman P, Gacias M, Weng Z, Chen H, Butovsky O. The TREM2-APOE pathway drives the transcriptional phenotype of dysfunctional microglia in neurodegenerative diseases. Immunity. 2017;47(3):566-581.e9. https://doi.org/10.1016/j.immuni.2017.08.008.
63. Liao Y, Smyth GK, Shi W. featureCounts: an efficient general purpose program for assigning sequence reads to genomic features. Bioinformatics. 2014;30(7):923–30. https://doi.org/10.1093/bioinformatics/btt656.
64. Loane DJ, Kumar A. Microglia in the TBI brain: the good, the bad, and the dysregulated. Exp Neurol. 2016;275:316–27. https://doi.org/10.1016/j.expneurol.2015.08.018.
65. Love MI, Huber W, Anders S. Moderated estimation of fold change and dispersion for RNA-seq data with DESeq2. Genome Biol. 2014;15(12):550. https://doi.org/10.1186/s13059-014-0550-8.
66. Maas AIR, Roozenbeek B, Manley GT. Clinical trials in traumatic brain injury: past experience and current developments. Neurotherapeutics. 2010. https://doi.org/10.1016/j.nurt.2009.10.022.
67. Malik A, Kanneganti T-D. Inflammasome activation and assembly at a glance. J Cell Sci. 2017;130(23):3955–63. https://doi.org/10.1242/jcs.207365.
68. McCarthy RC, Lu D-Y, Alkhateeb A, Gardeck AM, Lee C-H, Wessling-Resnick M. Characterization of a novel adult murine immortalized microglial cell line and its activation by amyloid-beta. J Neuroinflammation. 2016;13(1):21. https://doi.org/10.1186/s12974-016-0484-z.

69. McCarthy RC, Sosa JC, Gardeck AM, Baez AS, Lee C-H, Wessling-Resnick M. Inflammation-induced iron transport and metabolism by brain microglia. J Biol Chem. 2018;293(20):7853–63. https://doi.org/10.1074/jbc.RA118.001949.
70. McCrory P, Meeuwisse WH, Kutcher JS, Jordan BD, Gardner A. What is the evidence for chronic concussion-related changes in retired athletes: behavioural, pathological and clinical outcomes? Br J Sports Med. 2013;47(5):327–30. https://doi.org/10.1136/bjsports-2013-092248.
71. McKee AC, Cantu RC, Nowinski CJ, Hedley-Whyte ET, Gavett BE, Budson AE, Santini VE, Lee H-S, Kubilus CA, Stern RA. Chronic traumatic encephalopathy in athletes: progressive tauopathy after repetitive head injury. J Neuropathol Exp Neurol. 2009;68(7):709–35. https://doi.org/10.1097/NEN.0b013e3181a9d503.
72. Mckee AC, Daneshvar DH. The neuropathology of traumatic brain injury. Amsterdam: Elsevier; 2015. https://doi.org/10.1016/B978-0-444-52892-6.00004-0.
73. McKee AC, Stein TD, Nowinski CJ, Stern RA, Daneshvar DH, Alvarez VE, Lee H-S, Hall G, Wojtowicz SM, Baugh CM, Riley DO, Kubilus CA, Cormier KA, Jacobs MA, Martin BR, Abraham CR, Ikezu T, Reichard RR, Wolozin BL, Cantu RC. The spectrum of disease in chronic traumatic encephalopathy. Brain. 2013;136(1):43–64. https://doi.org/10.1093/brain/aws307.
74. Mehla J, Singh I, Diwan D, Nelson JW, Lawrence M, Lee E, Bauer AQ, Holtzman DM, Zipfel GJ. STAT3 inhibitor mitigates cerebral amyloid angiopathy and parenchymal amyloid plaques while improving cognitive functions and brain networks. Acta Neuropathol Commun. 2021;9(1):193. https://doi.org/10.1186/s40478-021-01293-5.
75. Mendiola AS, Ryu JK, Bardehle S, Meyer-Franke A, Ang KK-H, Wilson C, Baeten KM, Hanspers K, Merlini M, Thomas S, Petersen MA, Williams A, Thomas R, Rafalski VA, Meza-Acevedo R, Tognatta R, Yan Z, Pfaff SJ, Machado MR, Akassoglou K. Transcriptional profiling and therapeutic targeting of oxidative stress in neuroinflammation. Nat Immunol. 2020;21(5):513–24. https://doi.org/10.1038/s41590-020-0654-0.
76. Meng Q-Q, Feng Z-C, Zhang X-L, Hu L-Q, Wang M, Zhang H-F, Li S-M. PPAR- γ activation exerts an anti-inflammatory effect by suppressing the NLRP3 inflammasome in spinal cord-derived neurons. Mediat Inflamm. 2019;2019:1–12. https://doi.org/10.1155/2019/6386729.
77. Mira RG, Lira M, Cerpa W. Traumatic brain injury: mechanisms of glial response. Front Physiol. 2021. https://doi.org/10.3389/fphys.2021.740939.
78. Moore EL, Terryberry-Spohr L, Hope DA. Mild traumatic brain injury and anxiety sequelae: A review of the literature. Brain Inj. 2006. https://doi.org/10.1080/02699050500443558.
79. Moosecker S, Gomes P, Dioli C, Yu S, Sotiropoulos I, Almeida OFX. Activated PPARγ abrogates misprocessing of amyloid precursor protein tau missorting and synaptotoxicity. Front Cell Neurosci. 2019. https://doi.org/10.3389/fncel.2019.00239.
80. Moraes LA, Piqueras L, Bishop-Bailey D. Peroxisome proliferator-activated receptors and inflammation. Pharmacol Therap. 2006;110(3):371–85. https://doi.org/10.1016/j.pharmthera.2005.08.007.
81. Morin A, Mouzon B, Ferguson S, Paris D, Saltiel N, Browning M, Mullan M, Crawford F. A 3-month-delayed treatment with anatabine improves chronic outcomes in two different models of repetitive mild traumatic brain injury in hTau mice. Sci Rep. 2021. https://doi.org/10.1038/s41598-021-87161-7.
82. Mosure SA, Shang J, Eberhardt J, Brust R, Zheng J, Griffin PR, Forli S, Kojetin DJ. Structural basis of altered potency and efficacy displayed by a major in vivo metabolite of the antidiabetic PPARγ drug pioglitazone. J Med Chem. 2019;62(4):2008–23. https://doi.org/10.1021/acs.jmedchem.8b01573.
83. Mouzon B, Bachmeier C, Ojo J, Acker C, Ferguson S, Crynen G, Davies P, Mullan M, Stewart W, Crawford F. Chronic white matter degeneration, but no tau pathology at one-year post-repetitive mild traumatic brain injury in a tau transgenic model. J Neurotrauma. 2019;36(4):576–88. https://doi.org/10.1089/neu.2018.5720.
84. Mouzon BC, Bachmeier C, Ferro A, Ojo J-O, Crynen G, Acker CM, Davies P, Mullan M, Stewart W, Crawford F. Chronic neuropathological and neurobehavioral changes in a repetitive mild traumatic brain injury model. Ann Neurol. 2014;75(2):241–54. https://doi.org/10.1002/ana.24064.
85. Mouzon BC, Bachmeier C, Ojo JO, Acker CM, Ferguson S, Paris D, Ait-Ghezala G, Crynen G, Davies P, Mullan M, Stewart W, Crawford F. Lifelong behavioral and neuropathological consequences of repetitive mild traumatic brain injury. Ann Clin Transl Neurol. 2018;5(1):64–80. https://doi.org/10.1002/acn3.510.
86. Mouzon B, Chaytow H, Crynen G, Bachmeier C, Stewart J, Mullan M, Stewart W, Crawford F. Repetitive mild traumatic brain injury in a mouse model produces learning and memory deficits accompanied by histological changes. J Neurotrauma. 2012;29(18):2761–73. https://doi.org/10.1089/neu.2012.2498.
87. Musolino PL, Gong Y, Snyder JMT, Jimenez S, Lok J, Lo EH, Moser AB, Grabowski EF, Frosch MP, Eichler FS. Brain endothelial dysfunction in cerebral adrenoleukodystrophy. Brain. 2015;138(11):3206–20. https://doi.org/10.1093/brain/awv250.
88. Nair AB, Jacob S. A simple practice guide for dose conversion between animals and human. J Basic Clin Pharm. 2016;7(2):27–31. https://doi.org/10.4103/0976-0105.177703.
89. Nenov MN, Laezza F, Haidacher SJ, Zhao Y, Sadygov RG, Starkey JM, Spratt H, Luxon BA, Dineley KT, Denner L. Cognitive enhancing treatment with a PPARγ agonist normalizes dentate granule cell presynaptic function in Tg2576 APP mice. J Neurosci. 2014;34(3):1028–36. https://doi.org/10.1523/JNEUROSCI.3413-13.2014.
90. Nesto RW, Bell D, Bonow RO, Fonseca V, Grundy SM, Horton ES, Le Winter M, Porte D, Semenkovich CF, Smith S, Young LH, Kahn R. Thiazolidinedione use, fluid retention, and congestive heart failure. Circulation. 2003. https://doi.org/10.1161/01.CIR.0000103683.99399.7E.
91. Nicolakakis N. The nuclear receptor PPARγ as a therapeutic target for cerebrovascular and brain dysfunction in Alzheimer's disease. Front Aging Neurosci. 2010. https://doi.org/10.3389/fnagi.2010.00021.
92. Nonaka M, Chen X-H, Pierce J, Leoni MJ, Mcintosh TK, Wolf JA, Smith DH. Prolonged activation of NF-κB following traumatic brain injury in rats. J Neurotrauma. 1999;16(11):1023–34. https://doi.org/10.1089/neu.1999.16.1023.
93. Oh E, Kang J-H, Jo KW, Shin W-S, Jeong Y-H, Kang B, Rho T-Y, Jeon SY, Lee J, Song I-S, Kim K-T. Synthetic PPAR agonist DTMB alleviates alzheimer's disease pathology by inhibition of chronic microglial inflammation in 5xFAD mice. Neurotherapeutics. 2022;19(5):1546–65. https://doi.org/10.1007/s13311-022-01275-y.
94. Ojo JO, Bachmeier C, Mouzon BC, Tzekov R, Mullan M, Davies H, Stewart MG, Crawford F. Ultrastructural changes in the white and gray matter of mice at chronic time points after repeated concussive head injury. J Neuropathol Exp Neurol. 2015;74(10):1012–35. https://doi.org/10.1097/NEN.0000000000000247.
95. Ojo JO, Crynen G, Algamal M, Vallabhaneni P, Leary P, Mouzon B, Reed JM, Mullan M, Crawford F. Unbiased proteomic approach identifies pathobiological profiles in the brains of preclinical models of repetitive mild traumatic brain injury, tauopathy, and amyloidosis. ASN Neuro. 2020;12:175909142091476. https://doi.org/10.1177/1759091420914768.
96. Ojo JO, Mouzon B, Algamal M, Leary P, Lynch C, Abdullah L, Evans J, Mullan M, Bachmeier C, Stewart W, Crawford F. Chronic repetitive mild traumatic brain injury results in reduced cerebral blood flow, axonal injury, gliosis, and increased T-tau and tau oligomers. J Neuropathol Exp Neurol. 2016;75(7):636–55. https://doi.org/10.1093/jnen/nlw035.
97. Ojo J-O, Mouzon B, Greenberg MB, Bachmeier C, Mullan M, Crawford F. Repetitive mild traumatic brain injury augments tau pathology and glial activation in aged htau mice. J Neuropathol Exp Neurol. 2013;72(2):137–51. https://doi.org/10.1097/NEN.0b013e3182814cdf.
98. Ozen I, Ruscher K, Nilsson R, Flygt J, Clausen F, Marklund N. Interleukin-1 beta neutralization attenuates traumatic brain injury-induced microglia activation and neuronal changes in the globus pallidus. Int J Mol Sci. 2020;21(2):387. https://doi.org/10.3390/ijms21020387.
99. Pandolfo M, Reetz K, Darling A, Rodriguez de Rivera FJ, Henry P-G, Joers J, Lenglet C, Adanyeguh I, Deelchand D, Mochel F, Pousset F, Pascual S, Van den Eede D, Martin-Ugarte I, Vilà-Brau A, Mantilla A, Pascual M, Martinell M, Meya U, Durr A. Efficacy and safety of leriglitazone in patients with friedreich ataxia. Neurol Genetics. 2022. https://doi.org/10.1212/NXG.0000000000200034.
100. Pearson A, Ortiz C, Eisenbaum M, Arrate C, Browning M, Mullan M, Bachmeier C, Crawford F, Ojo JO. Deletion of PTEN in microglia ameliorates chronic neuroinflammation following repetitive mTBI. Mol Cell Neurosci. 2023. https://doi.org/10.1016/j.mcn.2023.103855.
101. Pedersen WA, McMillan PJ, Kulstad JJ, Leverenz JB, Craft S, Haynatzki GR. Rosiglitazone attenuates learning and memory deficits in Tg2576

Alzheimer mice. Exp Neurol. 2006;199(2):265–73. https://doi.org/10.1016/j.expneurol.2006.01.018.
102. Pérez-Segura I, Santiago-Balmaseda A, Rodríguez-Hernández LD, Morales-Martínez A, Martínez-Becerril HA, Martínez-Gómez PA, Delgado-Minjares KM, Salinas-Lara C, Martínez-Dávila IA, Guerra-Crespo M, Pérez-Severiano F, Soto-Rojas LO. PPARs and their neuroprotective effects in parkinson's disease: a novel therapeutic approach in α-synucleinopathy? Int J Mol Sci. 2023;24(4):3264. https://doi.org/10.3390/ijms24043264.
103. Prins M, Greco T, Alexander D, Giza CC. The pathophysiology of traumatic brain injury at a glance. Dis Models Mech. 2013. https://doi.org/10.1242/dmm.011585.
104. Prins ML, Alexander D, Giza CC, Hovda DA. Repeated mild traumatic brain injury: mechanisms of cerebral vulnerability. J Neurotrauma. 2013;30(1):30–8. https://doi.org/10.1089/neu.2012.2399.
105. Quinn DK, Mayer AR, Master CL, Fann JR. Prolonged postconcussive symptoms. Am J Psychiatry. 2018;175(2):103–11. https://doi.org/10.1176/appi.ajp.2017.17020235.
106. Ricote M, Glass C. PPARs and molecular mechanisms of transrepression. Biochim Biophys Acta BBA Mol Cell Biol Lipids. 2007;1771(8):926–35. https://doi.org/10.1016/j.bbalip.2007.02.013.
107. Risso D, Ngai J, Speed TP, Dudoit S. Normalization of RNA-seq data using factor analysis of control genes or samples. Nat Biotechnol. 2014;32(9):896–902. https://doi.org/10.1038/nbt.2931.
108. Rizzo FR, Musella A, De Vito F, Fresegna D, Bullitta S, Vanni V, Guadalupi L, Stampanoni Bassi M, Buttari F, Mandolesi G, Centonze D, Gentile A. Tumor necrosis factor and interleukin-1 β modulate synaptic plasticity during neuroinflammation. Neural Plast. 2018;2018:1–12. https://doi.org/10.1155/2018/8430123.
109. Rodríguez-Pascau L, Vilalta A, Cerrada M, Traver E, Forss-Petter S, Weinhofer I, Bauer J, Kemp S, Pina G, Pascual S, Meya U, Musolino PL, Berger J, Martinell M, Pizcueta P. The brain penetrant PPARγ agonist leriglitazone restores multiple altered pathways in models of X-linked adrenoleukodystrophy. Sci Transl Med. 2021. https://doi.org/10.1126/scitranslmed.abc0555.
110. Schimmel S, Acosta S, Lozano D. Neuroinflammation in traumatic brain injury: a chronic response to an acute injury. Brain Circ. 2017;3(3):135. https://doi.org/10.4103/bc.bc_18_17.
111. Searcy JL, Phelps JT, Pancani T, Kadish I, Popovic J, Anderson KL, Beckett TL, Murphy MP, Chen K-C, Blalock EM, Landfield PW, Porter NM, Thibault O. Long-term pioglitazone treatment improves learning and attenuates pathological markers in a mouse model of Alzheimer's disease. J Alzheimers Dis. 2012;30(4):943–61. https://doi.org/10.3233/JAD-2012-111661.
112. Semple RK. PPAR and human metabolic disease. J Clin Investig. 2006;116(3):581–9. https://doi.org/10.1172/JCI28003.
113. Serino A, Ciaramelli E, Di Santantonio A, Malagù S, Servadei F, Làdavas E. Central executive system impairment in traumatic brain injury. Brain Inj. 2006;20(1):23–32. https://doi.org/10.1080/02699050500309627.
114. Shibuya A, Wada K, Nakajima A, Saeki M, Katayama K, Mayumi T, Kadowaki T, Niwa H, Kamisaki Y. Nitration of PPARγ inhibits ligand-dependent translocation into the nucleus in a macrophage-like cell line, RAW 264. FEBS Lett. 2002;525(1–3):43–7. https://doi.org/10.1016/S0014-5793(02)03059-4.
115. Shie F-S, Nivison M, Hsu P-C, Montine TJ. Modulation of microglial innate immunity in Alzheimer's disease by activation of peroxisome proliferator-activated receptor gamma. Curr Med Chem. 2009;16(6):643–51. https://doi.org/10.2174/092986709787458399.
116. Siesjö BK, Siesjö P. Mechanisms of secondary brain injury. Eur J Anaesthesiol. 1996;13(3):247–68.
117. Simon DW, McGeachy MJ, Bayır H, Clark RSB, Loane DJ, Kochanek PM. The far-reaching scope of neuroinflammation after traumatic brain injury. Nat Rev Neurol. 2017;13(3):171–91. https://doi.org/10.1038/nrneurol.2017.13.
118. Simpson DSA, Oliver PL. ROS generation in microglia: understanding oxidative stress and inflammation in neurodegenerative disease. Antioxidants. 2020;9(8):743. https://doi.org/10.3390/antiox9080743.
119. Singh S, Singh TG. Role of nuclear factor kappa B (NF-κB) signalling in neurodegenerative diseases: an mechanistic approach. Curr Neuropharmacol. 2020;18(10):918–35. https://doi.org/10.2174/1570159X18666200207120949.
120. Stein DG. Embracing failure: what the phase III progesterone studies can teach about TBI clinical trials. Brain Inj. 2015;29(11):1259–72. https://doi.org/10.3109/02699052.2015.1065344.
121. Storer PD, Xu J, Chavis J, Drew PD. Peroxisome proliferator-activated receptor-gamma agonists inhibit the activation of microglia and astrocytes: implications for multiple sclerosis. J Neuroimmunol. 2005;161(1–2):113–22. https://doi.org/10.1016/j.jneuroim.2004.12.015.
122. Swanson KV, Deng M, Ting JPY. The NLRP3 inflammasome: molecular activation and regulation to therapeutics. Nat Rev Immunol. 2019;19(8):477–89. https://doi.org/10.1038/s41577-019-0165-0.
123. Heneka TM, Reyes-Irisarri E, Hull M, Kummer PM. Impact and therapeutic potential of PPARs in Alzheimers disease. Curr Neuropharmacol. 2011;9(4):643–50. https://doi.org/10.2174/157015911798376325.
124. Taylor CA, Bell JM, Breiding MJ, Xu L. Traumatic brain injury-related emergency department visits, hospitalizations, and deaths—United States, 2007 and 2013. MMWR Surveill Summ. 2017. https://doi.org/10.15585/mmwr.ss6609a1.
125. Thulasi Raman SN, Latreille E, Gao J, Zhang W, Wu J, Russell MS, Walrond L, Cyr T, Lavoie JR, Safronetz D, Cao J, Sauve S, Farnsworth A, Chen W, Shi P-Y, Wang Y, Wang L, Rosu-Myles M, Li X. Dysregulation of Ephrin receptor and PPAR signaling pathways in neural progenitor cells infected by Zika virus. Emerg Microb Infect. 2020;9(1):2046–60. https://doi.org/10.1080/22221751.2020.1818631.
126. Truett G, Heeger P, Mynatt R, Truett A, Walker J, Warman L. Preparation of PCR-quality mouse genomicDNA with hot sodiumhydroxide and tris (HotSHOT). Biotechniques. 2000;29:52–4.
127. Viswakarma N, Jia Y, Bai L, Vluggens A, Borensztajn J, Xu J, Reddy JK. Coactivators in PPAR-regulated gene expression. PPAR Res. 2010. https://doi.org/10.1155/2010/250126.
128. Wang BW, Hok V, Della-Chiesa A, Callaghan C, Barlow S, Tsanov M, Bechara R, Irving E, Virley DJ, Upton N, O'Mara SM. Rosiglitazone enhances learning, place cell activity, and synaptic plasticity in middle-aged rats. Neurobiol Aging. 2012;33(4):835.e13-835.e30. https://doi.org/10.1016/j.neurobiolaging.2011.08.013.
129. Wang Y-X. PPARs: diverse regulators in energy metabolism and metabolic diseases. Cell Res. 2010;20(2):124–37. https://doi.org/10.1038/cr.2010.13.
130. Warden A, Truitt J, Merriman M, Ponomareva O, Jameson K, Ferguson LB, Mayfield RD, Harris RA. Localization of PPAR isotypes in the adult mouse and human brain. Sci Rep. 2016;6(1):27618. https://doi.org/10.1038/srep27618.
131. Weinhofer I, Rommer P, Gleiss A, Ponleitner M, Zierfuss B, Waidhofer-Söllner P, Fourcade S, Grabmeier-Pfistershammer K, Reinert M-C, Göpfert J, Heine A, Yska HAF, Casasnovas C, Cantarín V, Bergner CG, Mallack E, Forss-Petter S, Aubourg P, Bley A, Berger J. Biomarker-based risk prediction for the onset of neuroinflammation in X-linked adrenoleukodystrophy. EBioMedicine. 2023;96:104781. https://doi.org/10.1016/j.ebiom.2023.104781.
132. Wen L, You W, Wang H, Meng Y, Feng J, Yang X. Polarization of microglia to the M2 phenotype in a peroxisome proliferator-activated receptor gamma-dependent manner attenuates axonal injury induced by traumatic brain injury in mice. J Neurotrauma. 2018;35(19):2330–40. https://doi.org/10.1089/neu.2017.5540.
133. Willis EF, Kim SJ, Chen W, Nyuydzefe M, MacDonald KPA, Zanin-Zhorov A, Ruitenberg MJ, Vukovic J. ROCK2 regulates microglia proliferation and neuronal survival after traumatic brain injury. Brain Behav Immun. 2024;117:181–94. https://doi.org/10.1016/j.bbi.2024.01.004.
134. Wofford K, Loane D, Cullen Dk. Acute drivers of neuroinflammation in traumatic brain injury. Neural Regen Res. 2019;14(9):1481. https://doi.org/10.4103/1673-5374.255958.
135. Wong R, Lénárt N, Hill L, Toms L, Coutts G, Martinecz B, Császár E, Nyiri G, Papaemmanouil A, Waisman A, Müller W, Schwaninger M, Rothwell N, Francis S, Pinteaux E, Denés A, Allan SM. Interleukin-1 mediates ischaemic brain injury via distinct actions on endothelial cells and cholinergic neurons. Brain, Behav Immun. 2019;76:126–38. https://doi.org/10.1016/j.bbi.2018.11.012.
136. Wright MB, Bortolini M, Tadayyon M, Bopst M. Minireview: challenges and opportunities in development of PPAR agonists. Mol Endocrinol. 2014;28(11):1756–68. https://doi.org/10.1210/me.2013-1427.
137. Wu J-S, Tsai H-D, Cheung W-M, Hsu CY, Lin T-N. PPAR-γ ameliorates neuronal apoptosis and ischemic brain injury via suppressing NF-κB-driven

p22phox transcription. Mol Neurobiol. 2016;53(6):3626–45. https://doi.org/10.1007/s12035-015-9294-z.
138. Yi HJ, Lee JE, Lee DH, Kim YI, Cho CB, Kim IS, Sung JH, Yang SH. The role of NLRP3 in traumatic brain injury and its regulation by pioglitazone. J Neurosurg. 2020. https://doi.org/10.3171/2019.6.JNS1954.
139. Yi J-H, Park S-W, Brooks N, Lang BT, Vemuganti R. PPARγ agonist rosiglitazone is neuroprotective after traumatic brain injury via anti-inflammatory and anti-oxidative mechanisms. Brain Res. 2008. https://doi.org/10.1016/j.brainres.2008.09.074.
140. Yu J, Chen T, Guo X, Zafar MI, Li H, Wang Z, Zheng J. The role of oxidative stress and inflammation in X-link adrenoleukodystrophy. Front Nutr. 2022. https://doi.org/10.3389/fnut.2022.864358.
141. Yu T-S, Tensaouti Y, Stephanz EP, Chintamen S, Rafikian EE, Yang M, Kernie SG. Astrocytic ApoE underlies maturation of hippocampal neurons and cognitive recovery after traumatic brain injury in mice. Commun Biol. 2021;4(1):1303. https://doi.org/10.1038/s42003-021-02841-4.
142. Zamanian MY, Taheri N, Opulencia MJC, Bokov DO, Abdullaev SY, Gholamrezapour M, Heidari M, Bazmandegan G. Neuroprotective and anti-inflammatory effects of pioglitazone on traumatic brain injury. Mediat Inflamm. 2022;2022:1–10. https://doi.org/10.1155/2022/9860855.
143. Zitnay GA. Lessons from national and international TBI societies and funds like NBIRTT. Vienna: Springer; 2005. https://doi.org/10.1007/3-211-27577-0_22.

Publisher's Note